1213965

RPP-RPT-50052, Rev. 0

Surface Geophysical Exploration of UPR-200-E-82 Near the C Tank Farm

Author Name: D. Rucker, hydroGEOPHYSICS, Inc.
Columbia Energy and Environmental Services, Inc.
Washington River Protection Solutions, LLC
Richland, WA 99352
U.S. Department of Energy Contract DE-AC27-08RV14800

EDT/ECN: DRF UC:
Cost Center: Charge Code:
B&R Code: Total Pages: 51

Key Words: SGE, surface Geophysical exploration, C tank farm, UPR-82

Abstract: A surface geophysical exploration survey that included direct current electrical resistivity was conducted at UPR-82 within the C Tank Farm on the Hanford Site. The survey included electrical current transmission and voltage measurements on 303 surface electrodes placed within a grid and 35 depth electrodes in five boreholes. The results showed that the past release was of sufficiently low conductivity as to not show a discernable feature in the geophysical image. Soil samples from a number of direct pushes also confirm the low conductivity.

TRADEMARK DISCLAIMER. Reference herein to any specific commercial product, process, or service by trade name, trademark, manufacturer, or otherwise, does not necessarily constitute or imply its endorsement, recommendation, or favoring by the United States Government or any agency thereof or its contractors or subcontractors.

JUL 13 2011
DATE:
STA: 15
HANFORD RELEASE
ID: 65

Nancy A Fouad 7/13/2011
Release Approval Date Release Stamp

Approved For Public Release

RECEIVED
MAY 17 2012
A-6002-767 (REV 3)
EDMC

EXECUTIVE SUMMARY

A surface geophysical exploration (SGE) survey was conducted over the UPR-82 release within the C tank farm on the Hanford Site. The survey focused on imaging the extents of the past release directly beneath the cesium pile. The survey included a concentrated three-dimensional (3D) analysis, with measurements on 303 surface electrodes placed within a grid and 35 depth electrodes in five boreholes, and a two-dimensional (2D) survey with three profile lines extending outside of the UPR-82 and C tank farm. The results of the 3D model showed a general distribution of high electrical resistivity values beneath the UPR-82 release, with values approximately two orders of magnitude higher than other sites where a discernable feature was noted in the resistivity data. Figure ES-1 shows a 3D rendered body of the resistivity results, demonstrating a resistive subsurface. Confirmation from sampled soil data also showed low porewater electrical conductivity values, with a maximum of 12 mS/cm and typical values less than 5 mS/cm. Other waste sites at Hanford, where resistivity has been extremely successful, display much higher porewater electrical conductivity (EC). The conclusion from the combined interpretation of porewater EC and electrical resistivity geophysics, therefore, is that there is no indication of a continuing source of groundwater contamination from this unplanned release.

Figure ES-1. 3D rendered resistivity values at UPR 82, view from southwest

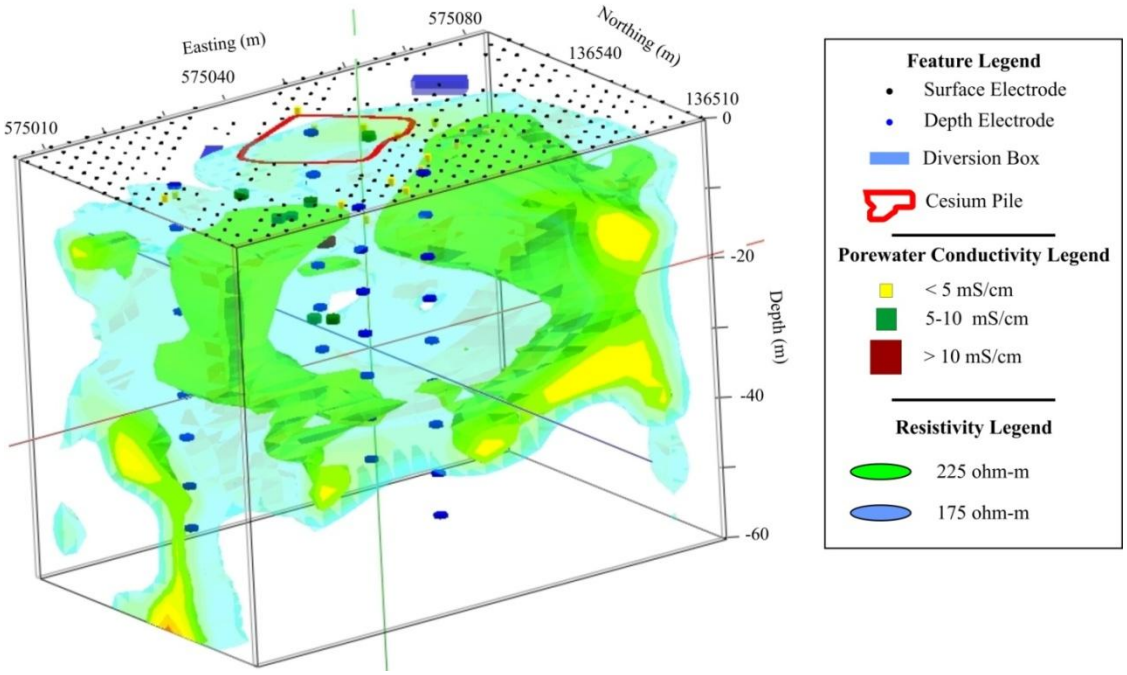

The second survey included a set of three long profile lines centered over the UPR 82 release to gain an understanding of potential groundwater impacts from the site. Unfortunately, the surface data were significantly impacted by the near surface infrastructure and no meaningful information could be discerned from the model results.

TABLE OF CONTENTS

1.0 INTRODUCTION 1-1
1.1 SCOPE 1-1
1.2 OBJECTIVES 1-1
1.3 REPORT LAYOUT 1-1

2.0 BACKGROUND 2-1
2.1 SITE DESCRIPTION 2-1
2.2 SUMMARY OF HYDROGEOLOGIC CONDITIONS 2-1
2.3 TANK CONTENTS 2-5
2.4 UNPLANNED RELEASES AT OR NEAR C TANK FARM 2-6
2.5 PAST CHARACTERIZATION OF C FARM 2-7
2.6 PAST CHARACTERIZATION OF UPR-82 2-11

3.0 DATA ACQUISITION AND PROCESSING METHODOLOGY 3-1
3.1 SURVEY DESIGN 3-1
3.2 EQUIPMENT 3-4
3.2.1 Electrode and Cable Layout 3-4
3.2.2 Resistivity Meter 3-6
3.3 ACQUISITION METHODOLOGY 3-6
3.4 DATA PROCESSING 3-7
3.4.1 3D Data Reduction 3-7
3.4.2 Depth Electrode Performance 3-9
3.4.3 Depth Electrode Data 3-12
3.4.4 2D Data Reduction 3-13
3.4.5 Inverse Modeling 3-16

4.0 MODELING RESULTS 4-1
4.1 3D POINT ELECTRODE MODELING 4-1
4.2 2D RESISTIVITY MODELING 4-5

5.0 CONCLUSIONS 5-1

6.0 REFERENCES 6-1

LIST OF FIGURES

1-1. Location of the C-Tank Farm and UPR-82 1-3
2-1. Location Map of Waste Management Area C and Surrounding Area and Cross-Section Lines shown in Figure 2-2 2-2
2-2. Subsurface Conditions in Vicinity of Waste Management Area C 2-3

2-3. Nitrate Concentrations (milligrams/liter) measured in ground water around C Tank Farm – June 2005 2-7
2-4. Results of Spectral Gamma Characterization of Drywells in C Farm, for Cesium-137 and Cobalt-60 2-8
2-5. Electrical Conductivity Measurements in Porewater Extracted from Soil Samples Taken around C Farm 2-10
2-6. Direct Push locations around UPR-82 2-11
2-7. Slant push locations and extracted samples 2-12
2-8. Porewater EC for push samples around UPR-82 2-13
3-1. Electrode Layout and the Local Distribution of Infrastructure for the UPR-82 3D Survey Area 3-2
3-2. Electrode Layout for the UPR-82 2D Survey Area 3-4
3-3. Resistivity Cable and Surface Electrode Layout 3-5
3-4. Remote Locations 3-7
3-5. 3D - Forward and Reverse Data Sets (Raw Data) 3-8
3-6. 3D - Forward and Reverse Data Sets after Data Editing 3-9
3-7. Performance Measure for Each of the Depth Electrodes 3-12
3-8. Transfer resistance (V/I) from depth electrodes for multiple projects 3-13
3-9. 2D Data Filtering Example 3-14
3-5. Data Reduction Statistics for the UPR-82 2D Resistivity Lines 3-14
3-10. Line 1 Normalized Potential (V/I) 3-15
4-1. Inverse model grid used for modeling the UPR-82 site 4-2
4-2. Plan View Depth Slices of Calculated Resistivity for Filtered Dataset 4-3
4-3. 3D rendered resistivity values at UPR 82 (view from southwest) 4-5
4-1. 2D Inverse Model Statistics 4-6
4-4. Line 1 2D Inverse Model 4-7
4-5. Line 2 2D Inverse Model 4-8
4-6. Line 3 2D Inverse Model 4-9

LIST OF TABLES

2-1. General Groundwater Flow Directions and Flow Rates for Single-Shell Tank Waste Management Area C in the 200 East Area 2-5
3-1. Depth Electrode Locations 3-2
3-2. 3D - Number of Data Points Retained During Data Editing Steps 3-9
3-3. Construction Details for UPR-82 Depth Electrodes 3-10
3-4. Depth Electrode Statistics for UPR-82 3-11

LIST OF TERMS

2D	two-dimensional
3D	three-dimensional
AGI	Advanced Geosciences, Inc
bgs	below ground surface
Columbia Energy	Columbia Energy and Environmental Services, Inc.
DOE	U.S. Department of Energy
EC	electrical conductivity
ft	foot
ft^3	cubic feet
gal	gallon
GPS	global positioning system
HFFACO	*Hanford Federal Facility Agreement and Consent Order*
HGI	hydroGEOPHYSICS, Inc.
kg	kilograms
L	liter
m	meter
mA	milliamp
MARS	Mobile Arm Retrieval System
PUREX	plutonium-uranium extraction
RCRA	*Resource Conservation and Recovery Act of 1976*
RMS	root-mean-square
SGE	surface ground exploration
SST	single-shell tank
UPR	unplanned release
WMA	waste management area
WRPS	Washington River Protection Solutions, LLC

1.0 INTRODUCTION

This report documents surface geophysical exploration (SGE) activities completed within a 78-meter by 51-meter area surrounding the unplanned release site (UPR) UPR-82 in the vicinity of the C tank farm at the U.S. Department of Energy (DOE) Hanford Site in Washington State. hydroGEOPHYSICS, Inc. (HGI) and Columbia Energy and Environmental Services, Inc. (Columbia Energy), with support from technical staff of Washington River Protection Solutions, LLC (WRPS), conducted a three-dimensional (3D) survey of the subsurface using electrical resistivity. Data acquisition and analysis were performed in accordance with RPP-PLAN-39364, *Work Plan for Surface Geophysical Exploration of UPRs near the C Tank Farm.* High-resolution electrical resistivity data were acquired using both surface electrodes (located at the ground surface) and depth electrodes completed within the UPR-82 footprint.

1.1 SCOPE

The scope of this electrical resistivity characterization survey included:

- Data acquisition on both surface electrodes and depth electrodes
- Data processing that included the use of methods and controls to ensure quality in the processing and reduction of data collected
- Data visualization that included contouring of resistivity data from the 3D acquired data set
- Compilations of 3D resistivity cross sections.

The UPR-82 is immediately north and west of both UPR-81 and UPR-86, which were investigated in 2009 and 2010, respectively, using electrical resistivity (RPP-RPT-41236, *Surface Geophysical Exploration of UPR 200-E-81 Near the C Tank Farm;* RPP-RPT-47486, *Surface Geophysical Exploration of UPR 200-E-86 Near the C Tank Farm*). Figure 1-1 shows the locations of the site.

1.2 OBJECTIVES

The main objective for this geophysical investigation was to collect and analyze electrical resistivity data to identify low resistivity regions in and around the UPR-82 site in the vicinity of the C tank farm area. Low resistivity measurements are indicative of increased moisture content, changes in geologic composition or formations, or increased concentration of electrolytes compared to background conditions. It was hoped that the survey would identify the distribution and magnitude of the unplanned release at the site.

1.3 REPORT LAYOUT

The overall scope and content of this report is divided into several main sections as follows:

- **Section 1.0, Introduction** – Describes the scope and objectives of the investigation.

- **Section 2.0, Background** – Describes the setting and information regarding the C tank farm and the UPR-200-E- 82 unplanned release.
- **Section 3.0, Data Acquisition and Processing** – Presents the general layout for the data acquisition and processing, with methods and controls used to ensure the quality and control of data collection, reduction, and processing used in this study.
- **Section 4.0, Results and Interpretations** – Presents the results from the electrical resistivity surveying effort and an interpretation of the resistivity measurements including the results of the inversion analysis.
- **Section 5.0, Conclusions and Recommendations** – Provides a summary and conclusions drawn from the results and interpretations. Recommendations are provided to improve quality for future investigations.
- **Section 6.0, References** – Provides a listing of references cited in the report.

Figure 1-1, location of the C tank farm and UPR-82, shows:

a. Overhead photo of the C tank farm.

b. Location of the C tank farm within the Hanford Site.

c. Infrastructure map of the C tank farm and UPR-82 survey area.

Figure 1-1. Location of the C-Tank Farm and UPR-82.

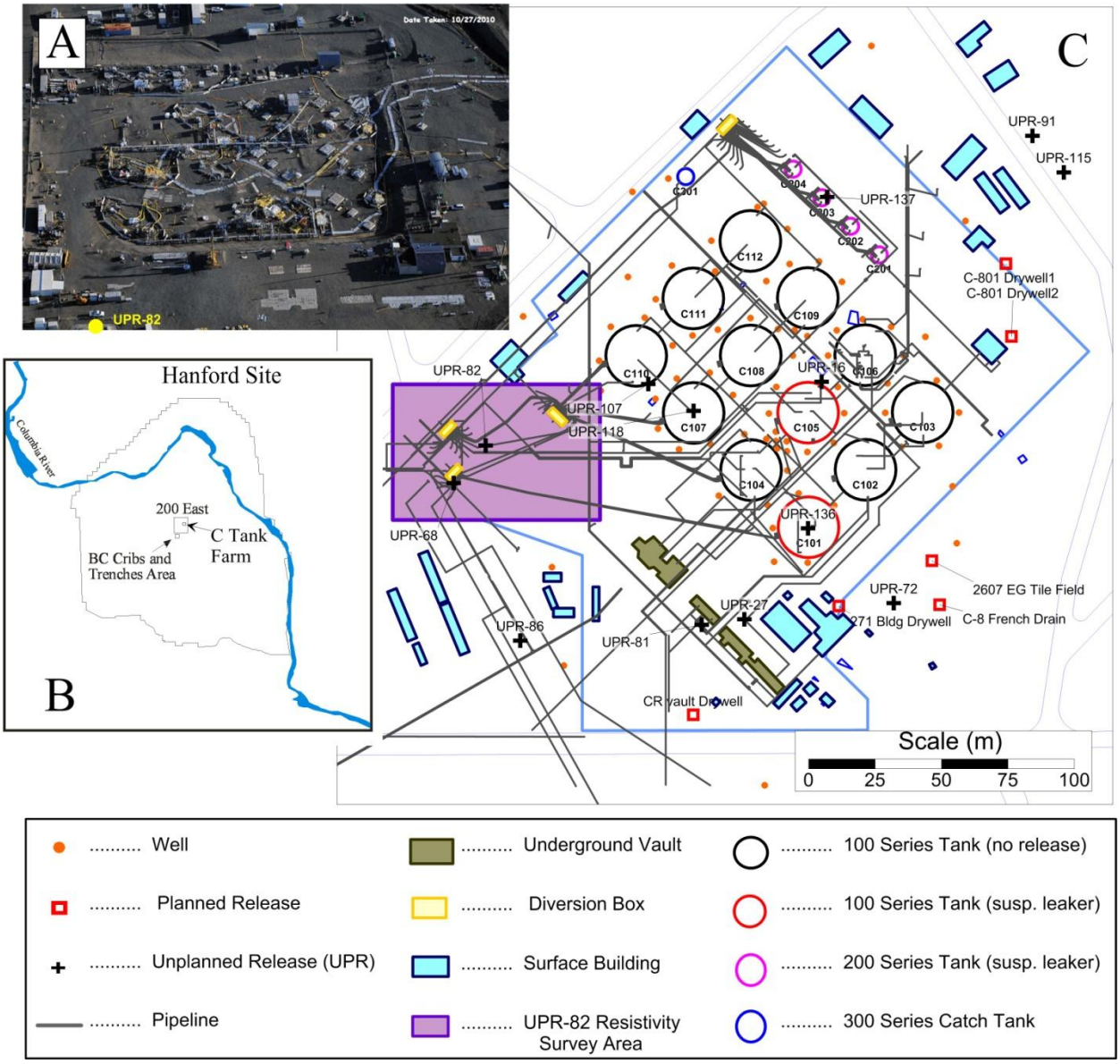

2.0 BACKGROUND

2.1 SITE DESCRIPTION

C farm is located in the Central Plateau, near the eastern edge of the 200 East Area (Figure 1-1). It was one of the first tank farms built, between 1944 and 1945. The tank farm contains twelve 100-series tanks, four 200-series tanks, and one 300-series catch tank (see Figure 2-1). The 100-series tanks are 23 meters (m) (75 feet [ft]) in diameter, with a 5-m (15-ft) operating depth, and an operating capacity of 2,006,000 liters (L) (530,000 gallons [gal]) each. The 200-series tanks are 6 m (20 ft) in diameter, with a 7.32-m (24-ft) operating depth, and an operating capacity of 208,000 L (55,000 gal) each. The C-301 catch tank has a capacity of 136,000 L (36,000 gal). Only single-shell tanks (SST) 241-C-101 (C-101) through 241-C-106 (C-106) have concrete pits. The other 100-series tanks are equipped with centrally located salt well pump pits. The tanks sit below grade with at least 2 m (7 ft) of soil cover to provide shielding from radiation exposure to operating personnel. Tank pits are located on top of the tanks and provide access to the tank, pumps, and monitoring equipment.

To support the transfer and storage of waste within waste management area (WMA) C SSTs, there is a complex waste transfer system of pipelines (transfer lines), diversion boxes, vaults, valve pits, and other miscellaneous structures.

Twelve UPRs have occurred within or near C farm. The largest ones are associated with leaks in pipelines or diversion boxes, from inlet/outlet ports of the SSTs, or with leaks from the SSTs themselves. RPP-PLAN-39114, *Phase 2 RCRA Facility Investigation/Corrective Measures Study Work Plan for Waste Management Area C*, provides more detail on these UPR sites. This study focuses on the UPR-82, in the western portion of the site.

Six planned releases have also occurred within the tank farm, which include a septic discharge, drywells, and a French drain. Figure 2-1 shows the approximate location of all planned and unplanned releases.

Five SSTs (C-103, C-201, C-202, C-203, and C-204) have been retrieved to meet the requirements of *Hanford Federal Facility Agreement and Consent Order* (HFFACO) (Ecology et al. 1989). SST C-106 also has been retrieved, but is undergoing a HFFACO Appendix H waiver request, as its residual waste volume (370 cubic feet [ft^3] [RPP-19866, *Calculation for the Post-Retrieval Waste Volume Determination for Tank 241-C-106*]) is above the HFFACO limit of 360 ft^3. SSTs C-108, C-109, and C-110 are currently undergoing waste retrieval activities (HNF-EP-0182, *Waste Tank Summary Report for Month Ending April 30, 2009*). Activities related to waste retrieval at SSTs C-104 and C-111 have been started. Preparations are underway to initiate waste retrieval at SST C-107 using the Mobile Arm Retrieval System (MARS).

2.2 SUMMARY OF HYDROGEOLOGIC CONDITIONS

The hydrogeological framework underlying WMA C and vicinity is well understood and is the result of several decades of site characterization activities, described in numerous reports (HW-61780, *Subsurface Geology of the Hanford Separation Areas;* ARH-LD-132, *Geology of the 241-C Tank Farm*; RPP-14430, *Subsurface Conditions Description of the C and A-AX Waste*

Management Area; and RPP-35484, *Field Investigation Report for Waste Management Areas C and A-AX*).

Figure 2-1. Location Map of Waste Management Area C and Surrounding Area and Cross-Section Lines shown in Figure 2-2.

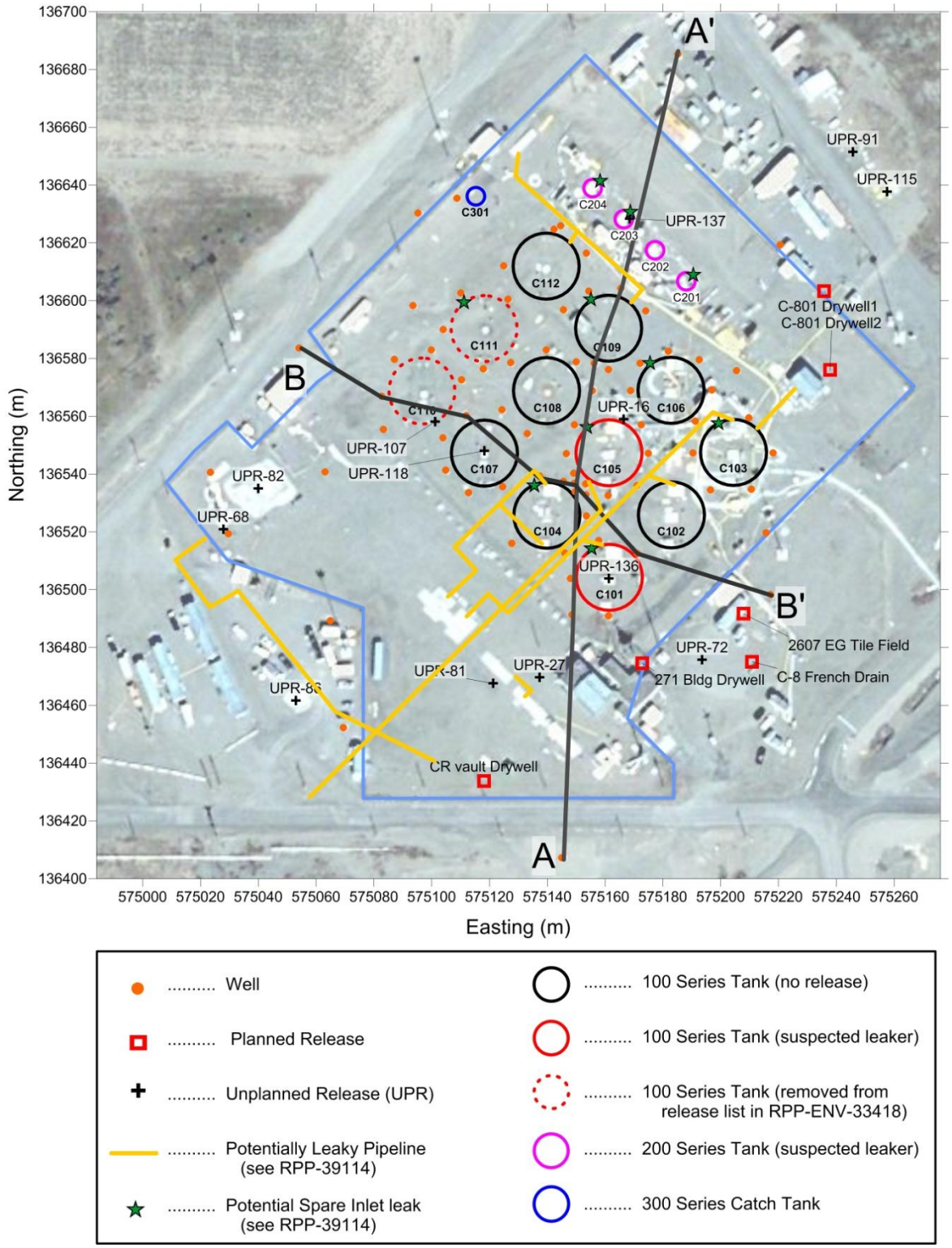

Figure 2-2. Subsurface Conditions in Vicinity of Waste Management Area C.

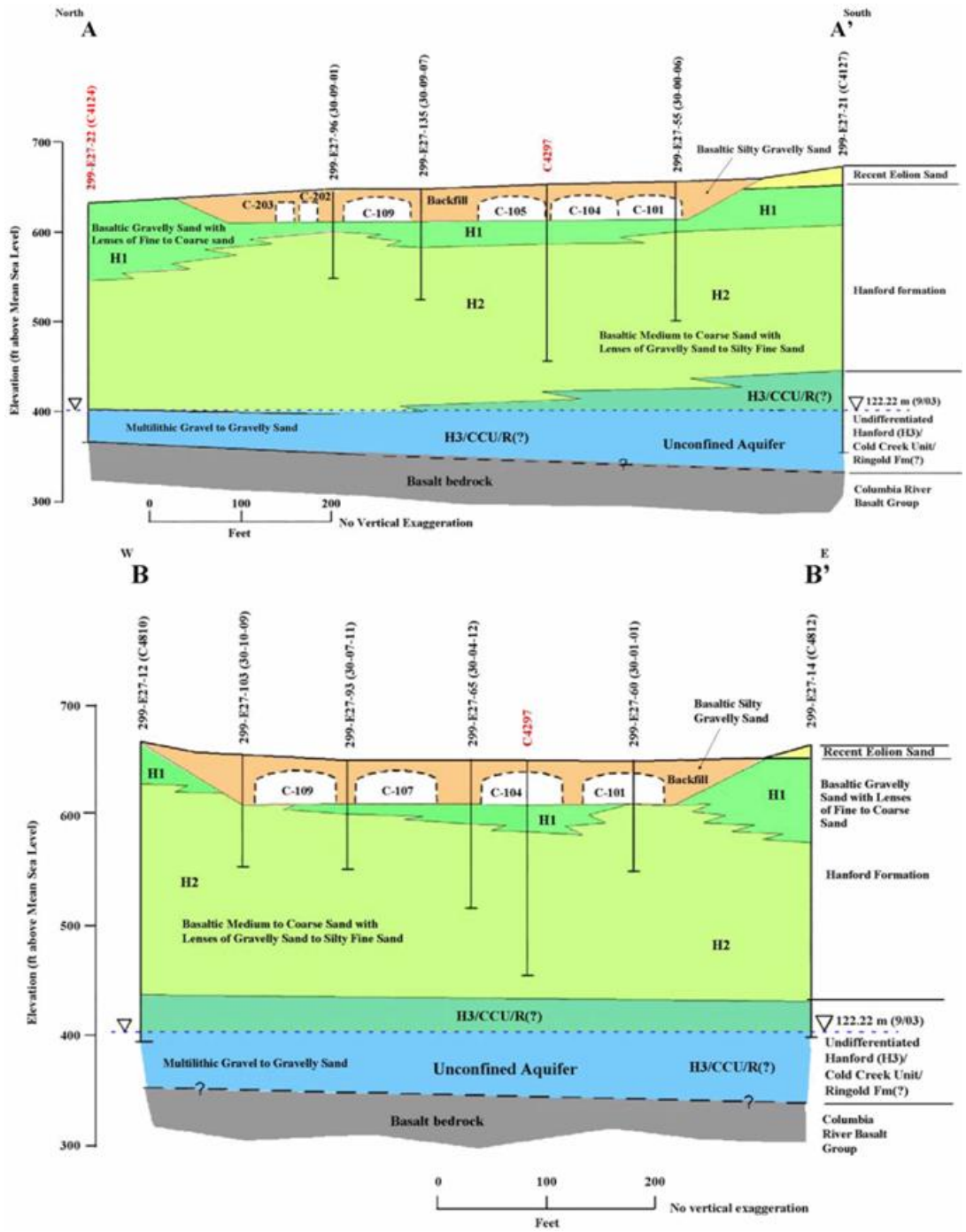

The main source of information on the geologic strata underlying the Hanford Site and tank farms is data obtained from drilling boreholes and subsequent analyses of the sediments and contaminants within them (e.g., PNNL-14656, *Borehole Data Package for Four CY 2003 RCRA Wells 299-E27-4, 299-E27-21, 299-E27-22, and 299-E27-23 at Single-Shell Tank, Waste*

Management Area C, Hanford Site, Washington). More detailed discussion of the borehole-specific geologic and geochemical characteristics of the WMA C vadose zone are provided in RPP-23748, *Geology, Hydrogeology, Geochemistry, and Mineralogy Data Package for the Single-Shell Tank Waste Management Areas at the Hanford Site* and PNNL-15955, *Geology Data Package for the Single-Shell Tank Waste Management Areas at the Hanford Site*.

Three major stratigraphic units underlie C farm, which include in ascending order:

1. The igneous Columbia River Basalt Group and two sedimentary interbed units.
2. The undifferentiated H3 unit of the Hanford formation/Cold Creek unit/Ringold Formation (H3/CCU/RF).
3. The Hanford formation (RPP-PLAN-39114).

A general representation of the lateral and vertical distribution of these three units near WMA C along north-south and west-east sections is illustrated in Figure 2-2. The undifferentiated H3/CCU/RF unit directly above the Columbia River Basalt Group is labeled as undifferentiated because two or three major stratigraphic units may have commingled, and clear distinctions between them cannot be made. These include the H3 subunit of the Hanford formation, the Cold Creek unit, and the Ringold Formation's Wooded Island member. The vadose zone is comprised of the backfill, Hanford formation, and the undifferentiated H3/CCU/RF unit.

Overall, the vadose zone is 250 to 260 ft thick at WMA C (Figure 2-2). The water table and the associated unconfined aquifer occurs within the H3/CCU/RF unit and the overall thickness of this aquifer ranges from approximately 55 ft at well 299-E27-155 (south of WMA C) to approximately 38 ft at well 299-E27-22 (north of WMA C).

All major hydrogeological units are inferred to be essentially continuous in this area, although unit thicknesses vary and some subunits are not continuous. General characteristics of each unit beneath WMA C are described more fully in RPP-PLAN-39114, Section 2.3.1. Finally, backfill materials, consisting of poorly sorted cobbles, pebbles, and coarse to medium sand derived from the H1 subunit of the Hanford formation, are distributed around the SSTs and tank infrastructure.

Both water level and general direction of groundwater flow in this region have been altered many times throughout Hanford Site operations history by high-volume wastewater discharges to various ponds (DOE/RL-2008-01, *Hanford Site Groundwater Monitoring for Fiscal Year 2007*; PNNL-16346, *Hanford Site Groundwater Monitoring for Fiscal Year 2006*).

In the 1980s, a groundwater mound in this area was maintained by liquid discharge to B Pond to the east of WMA C, elevating the water table and imposing a southwestern trend in groundwater flow under WMA C (PNNL-15837, *Data Package for Past and Current Groundwater Flow and Contamination Beneath Single-Shell Tank Waste Management Areas*).

Between 1944 and the mid-1990s, the volume of artificial recharge from Hanford Site operations wastewater disposal was significantly greater than recharge from precipitation. An estimated 1.68×10^{12} L (4.44×10^{11} gal) of liquid was discharged to disposal ponds, trenches, and cribs during this period. Wastewater discharge has decreased since 1984 and currently contributes a volume of recharge in the same range as the estimated natural recharge from precipitation. Because of the reduction in discharges, groundwater levels are falling, particularly around the operational areas (PNNL-15070, *Hanford Site Groundwater Monitoring for Fiscal Year 2004*).

Current general groundwater flow directions and general flow rates are given in Table 2-1 for WMA C (as adapted from PNNL-15670, *Hanford Site Groundwater Monitoring for Fiscal Year 2005*). The general flow rate has remained unchanged since fiscal year 2005. The water table is very flat over all of the 200 East Area and the current groundwater flow direction is to the southwest to south-southwest with a flow rate, based on migration of sulfate, of 0.09 m per day (DOE/RL-2008-01).

Table 2-1. General Groundwater Flow Directions and Flow Rates for Single-Shell Tank Waste Management Area C in the 200 East Area.

Waste Management Area	Groundwater Flow Direction	Gradient	Groundwater Flow Rate[a,b] (m/day)
C	SW – SSW	0.0001	0.7 to 2.4

Data in table originally reported in PNNL-15670.
Table 2-2 from RPP-PLAN-39114.
[a] Groundwater flow rates are calculated using the Darcy equation.
[b] The multi-stress slug test was used for the calculation of groundwater flow rate for Waste Management Area C.

2.3 TANK CONTENTS

The C tank farm received waste generated by essentially all of the major chemical processing operations that occurred at the Hanford Site, including bismuth phosphate fuel processing, uranium recovery, plutonium-uranium extraction (PUREX) fuel processing, fission product recovery, and tank farm interim stabilization and isolation activities. Only the C tank farm was operational during the bismuth phosphate and uranium recovery processes (RPP-14430).

The C tank farm, constructed between 1943 and 1944, began receiving the first metal and cycle waste from B plant in 1946. Ultimately, SSTs C-101 through C-106 received metal waste and SSTs C-107 through C-112 received first cycle waste. All SSTs were filled with bismuth phosphate waste by the end of 1948. The 200 series SSTs also received metal waste. In 1952, to free up tank space, first cycle waste was transferred to the 242-B evaporator.

Metal waste was also removed from C tank farm beginning in 1952 and transferred to U Plant for uranium recovery. Ancillary equipment involved in the metal waste transfer included the 244-CR vault and diversion boxes 241-CR-151, -152 and –153. Subsequently, tributyl phosphate waste, a byproduct of the uranium recovery process, was returned to C tank farm. The 244-CR vault was modified in 1955 to scavenge tributyl phosphate waste (that is, to separate cesium-137 from the supernatant by precipitation) present in SSTs C-107 through C-112. The scavenged slurry was redeposited in SSTs C-109 and C-112 to settle and the resultant supernatant was discharged to the BC cribs, located about 2 miles (3.2 kilometers) to the south.

The tanks in the C tank farm currently contain an estimated total volume of 1.5 million gal (5.68×10^6 L) of mixed wastes consisting of various bismuth phosphate, reduction-oxidation, and PUREX processing waste streams (HNF-EP-0182). General tank content (i.e., liquid and

solid volumes) data and some tank monitoring data are summarized monthly in waste tank summary reports (e.g., HNF-EP-0182).

2.4 UNPLANNED RELEASES AT OR NEAR C TANK FARM

There have been a number of unplanned releases reported in and around the C tank farm. A description of these unplanned releases are given in RPP-RPT-42294 *Hanford Waste Management Area C Soil Contamination Inventory Estimates*. The largest unplanned releases were associated with transfer of PUREX waste around 1970, and occurred near diversion boxes 241-CR-151, 241-C-151, and 241-C-152 (UPR-81, UPR-82, and UPR-86, respectively). Estimated losses ranged from 2,600 to 36,000 gal (9,800 to 136,000 L). UPR-136 is associated with the SST C-101, which is estimated at approximately 17,000 to 24,000 gal (64,000 to 90,000 L). The remaining eight unplanned releases were primarily small surface spills and airborne contamination.

Although the radiological inventory associated with UPR-81, near the 241-CR-151 diversion box, was a reasonably low activity waste stream, it contained approximately 17,000 pounds (7,700 kilograms [kg]) of NO_3/NO_2 combined (RPP-15317, *241-C Waste Management Area Inventory Data Package*).

UPR-82 was a waste-loss event near the 241-C-152 diversion box that occurred in December 1969 and involved the loss of approximately 2,600 gallons of cesium-137 recovery process feed solution (Wood et al. 2003). The leak event created a temporary ground-surface puddle measuring 100 gallons in volume, which was quickly covered over with clean gravel. It is estimated that 11,300 Ci of cesium-137, 18.3 kg of uranium, and 5.01 Ci of technetium-99 were released to the subsurface (PNNL-15617, *Characterization of Vadose Zone Sediments from C Waste Management Area: Investigation of the C-152 Transfer Line Leak*).

An overall assessment of the spectral gamma logging data from C farm drywells suggests that most vadose zone contamination in the tank farm originated from surface or near surface sources. This is demonstrated by relatively high concentrations of cesium-137 in the near surface and a general decrease in cesium-137 activity with depth. Cobalt-60 is found near the bottom of many of the drywells that manifest below near- surface cesium-137 contamination. This indicates that “mobile” cobalt-60 was actively transported down via subsequent recharge water (rain and snow melt). These contamination events were generally not associated with recorded events and are comparatively insignificant sources of vadose zone contamination.

The C tank farm is currently in *Resource Conservation and Recovery Act of 1976* (RCRA) groundwater assessment monitoring. Contaminants present in the groundwater along with potential contamination sources are discussed in PNNL-15670. Figure 2-3 shows the distribution of nitrate obtained from 2005 groundwater data (PNNL-15670). At Hanford, nitrate migrates through the soil practically unimpeded, providing a maximum bound for resistivity imaging. The nitrate concentrations in the vicinity of C tank farm are considerably lower than those measured in tank farm areas previously assessed with SGE (S farm, U farm, and B complex).

Figure 2-3. Nitrate Concentrations (milligrams/liter) measured in ground water around C Tank Farm – June 2005.

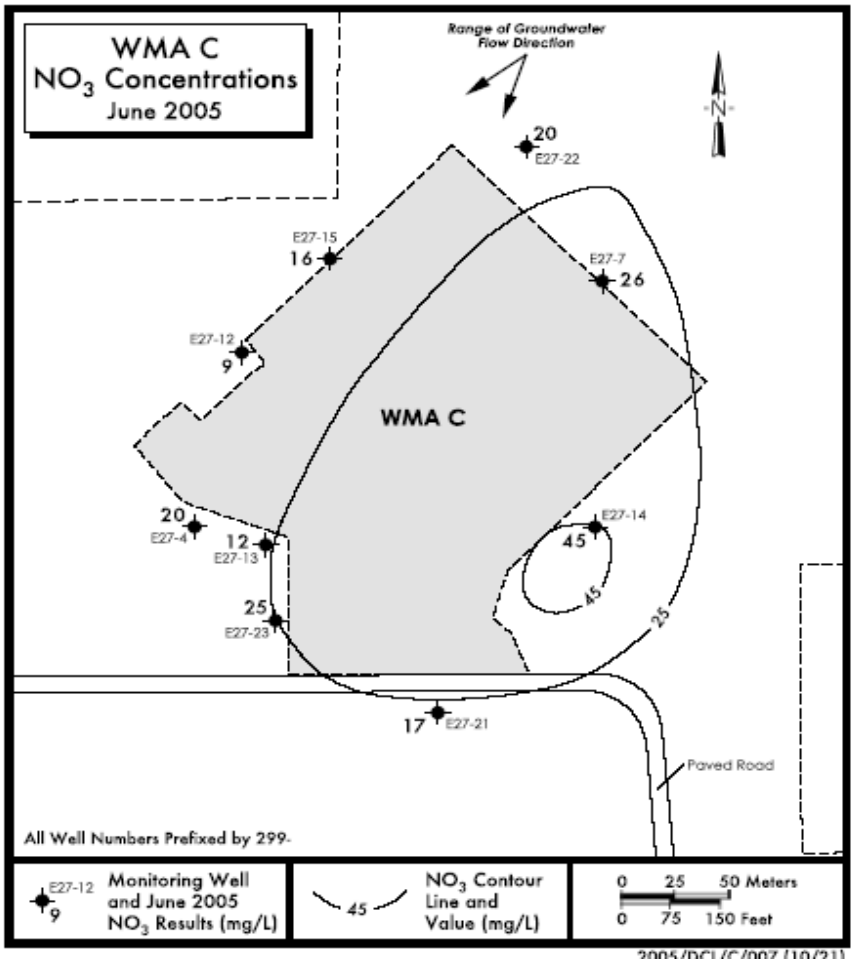

Source: RPP-16608, *Site-Specific Single-Shell Tank Phase 1 RCRA Facility Investigation/Corrective Measures Study Work Plan Addendum for Waste Management Areas C, A-X, and U.*

2.5 PAST CHARACTERIZATION OF C FARM

A broad range of characterization data and information exists for the C tank farm, including results from geophysical logging of wells and direct pushes (spectral gamma, gross gamma, and neutron), direct soil sampling of vadose zone sediments, and groundwater sampling. A baseline of geophysical logging was performed on 70 drywells around the tanks in 1997. An update for the geophysical logging is planned for 48 of these wells, as described in the Phase 2 work plan (RPP-PLAN-39114). Specific results from spectral gamma logging in the 1997 study are shown in Figure 2-4. These results display dry well locations where activity levels of cesium-137 greater than 100 pCi/g, greater than 10 pCi/g, and greater than 1 pCi/g were detected.
In addition, the results indicate the dry well locations where logging detected cobolt-60 greater than 1 pCi/g. A separate symbol is used to indicate each of the threshold levels for both cesium-137 and cobalt-60. These measurements suggest that notable areas of contamination can

be found near C-101, C-103, C-104, C-105, C-106, and C-109. In a few of the dry well locations, multiple peaks of cesium-137 with depth are indications of the possible occurrence of multiple leak events over time.

Figure 2-4. Results of Spectral Gamma Characterization of Drywells in C Farm, for Cesium-137 and Cobalt-60.

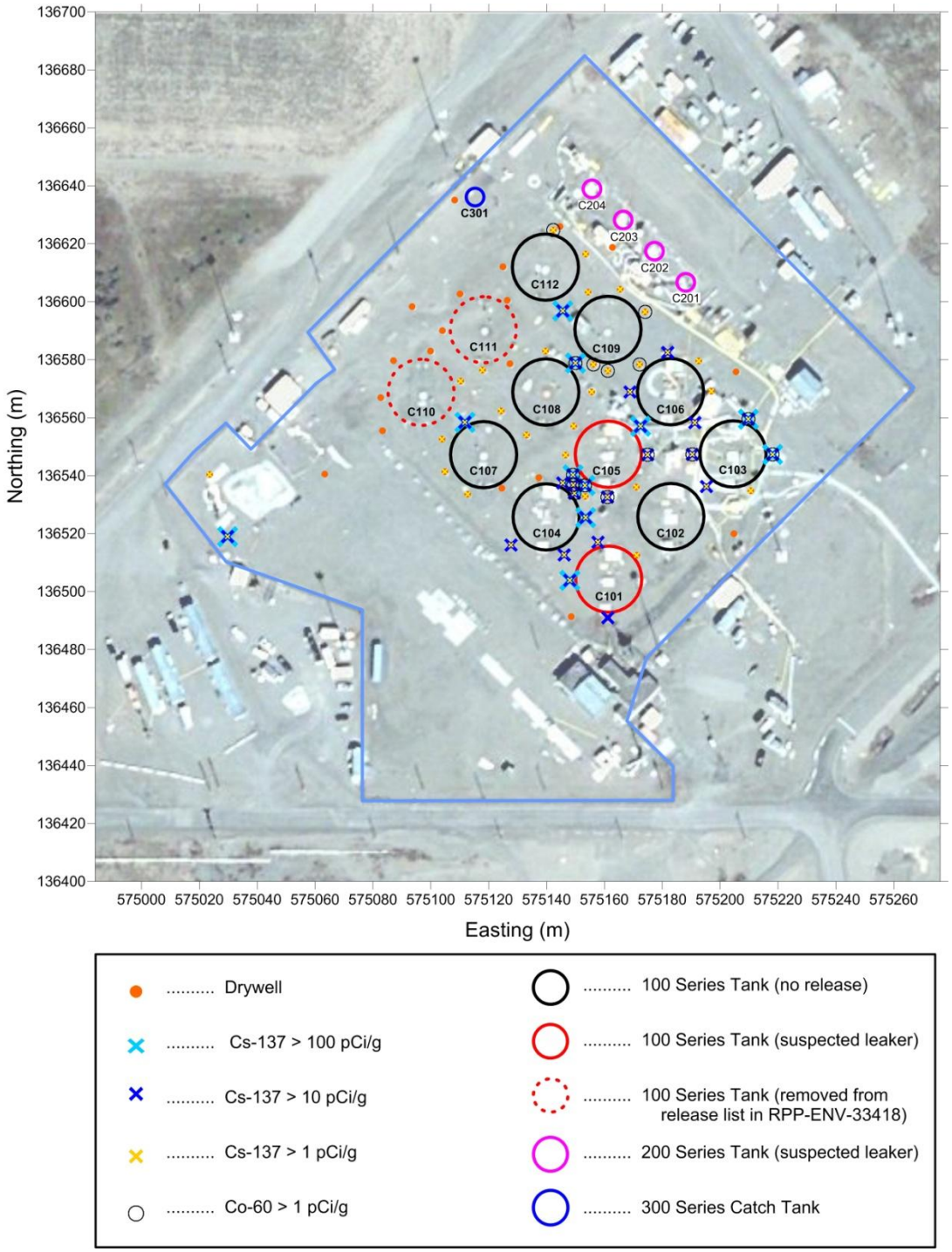

Data from 1997 logging event.

Figure 2-5 shows the distribution of borehole locations where soil samples have been taken. In most cases, pore water samples were extracted and analyzed from only a few soil samples for each borehole. However, borehole C4297 (with 144 samples from 2 to 195 ft below ground surface) located to the northeast of SST C-104 and well 299-E27-22 (with 110 samples from 19 to 230 ft below ground surface) located to the north of the C farm fence line are exceptions. The majority of electrical conductivity (EC) values measured in pore water samples display values less than 5 mS/cm (or 2 ohm-m). Results from a few samples, in particular near the UPR-82 release site, display high EC values. The highest readings for EC came from pore water extracted from samples from a depth of 42 ft (12.7 mS/cm) at slant direct push location, C5105; from a depth of 61.5 ft (25 mS/cm) in borehole C4297, and from a depth of 28 ft (20.1 mS/cm) in well 299-E27-22. Most direct push borehole locations at UPR-81 did not have accompanying EC data, but had significant measured nitrate concentrations. This included a value of 199 µg /g at a depth of 42.5 ft, in direct push location C6394. The maximum nitrate values measured near UPR-86 was 21.4 µg /g at a depth of 18 ft, in direct push location C5960. Similarly, the samples taken near SST C-103 show elevated nitrate values of 90.3 and 192 µg/g at depths of 114 ft and 125 ft in direct push locations C7466 and C7468, respectively.

Figure 2-5. Electrical Conductivity Measurements in Porewater Extracted from Soil Samples Taken around C Farm.

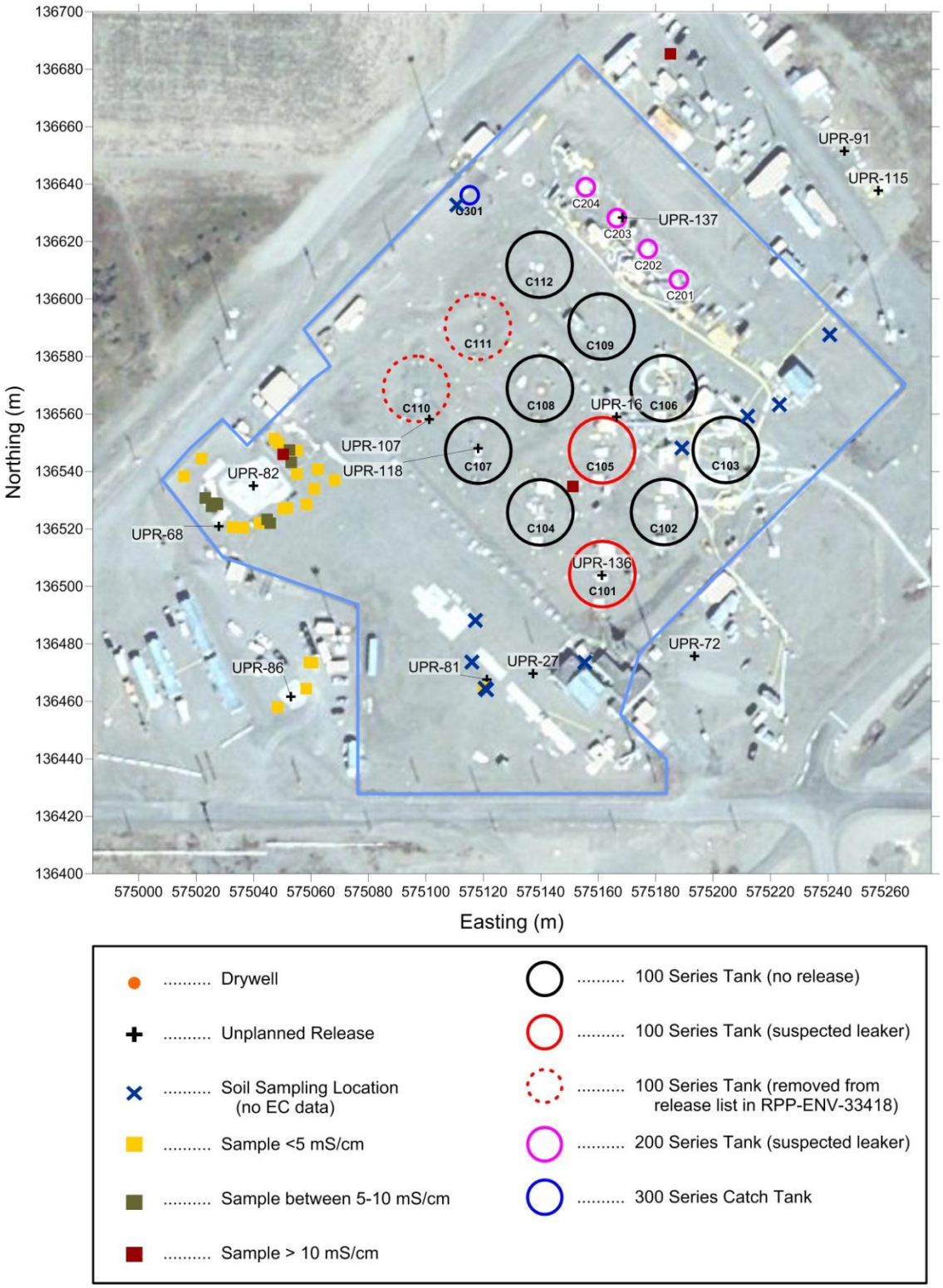

2.6 PAST CHARACTERIZATION OF UPR-82

An initial geological/geochemical investigation in the vicinity of UPR-200-E-82 was performed using pairs of direct-push probe holes. A total of 41 vertical direct pushes extending to approximately 60 ft below ground surface (bgs) were completed between July and September, 2005, to characterize vadose zone moisture and the distribution of contaminants. Twenty vadose zone sediment sample sets, containing one or two core samples in stainless-steel liners and one grab sample, were delivered to the laboratory for characterization and analysis. The sediments were collected around the documented location of the C-152 pipeline leak (UPR-200-E-82) and created an approximately 120-ft-diameter circular pattern around the waste site (PNNL-15617). Figure 2-6 shows the sites for the direct pushes.

Figure 2-6. Direct Push locations around UPR-82.

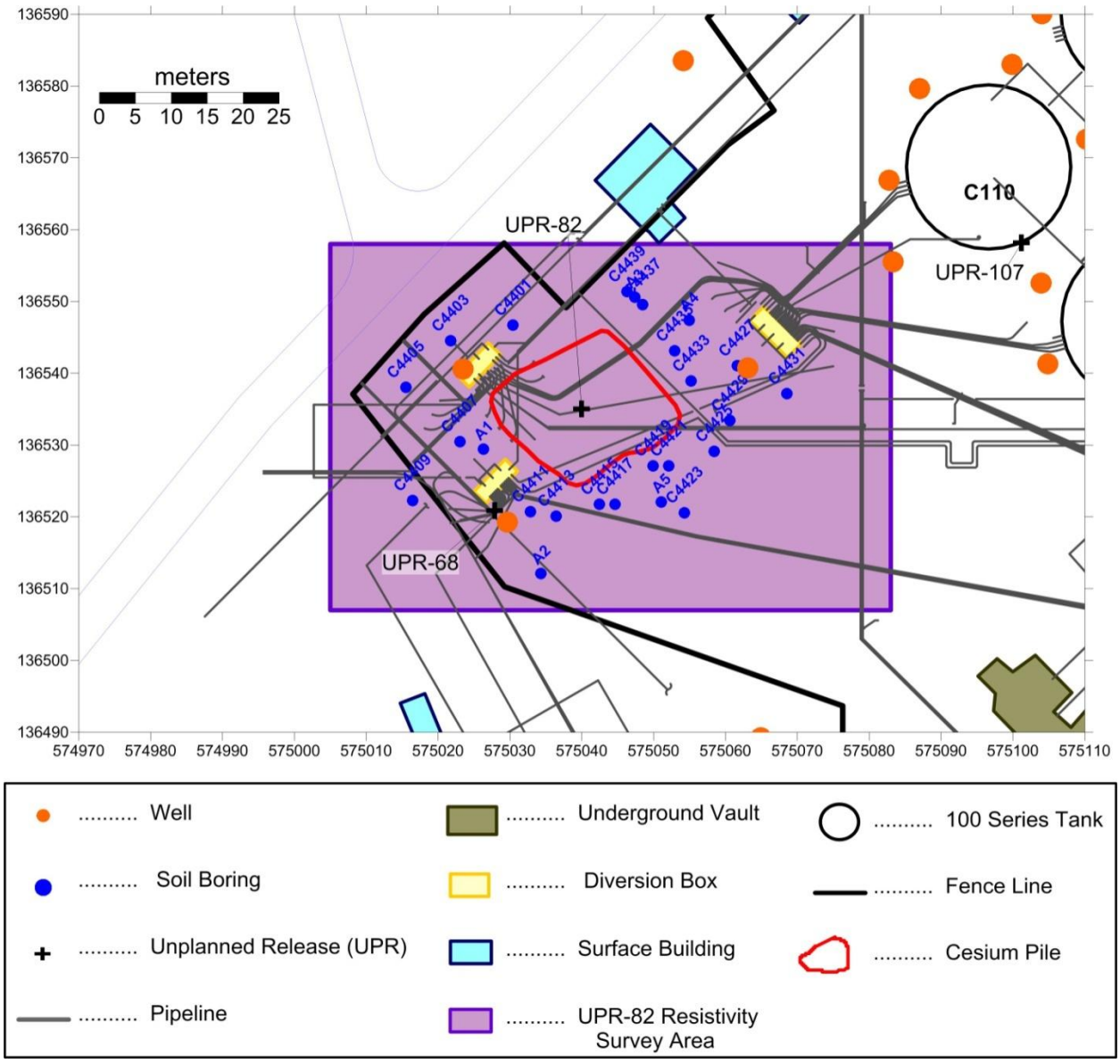

A second series of six probe holes were emplaced around the site of the pipeline leak between March and June, 2006. These probe holes were driven at angles of 30º, 45º, or 60º from horizontal, and extended to approximately 80 ft bgs. Up to three sets of samples (1.5 ft of core plus material recovered from the drive shoe) were retrieved from each slant probe hole (PNNL-15617). Figure 2-7 shows the locations of the samples.

Figure 2-7. Slant push locations and extracted samples.

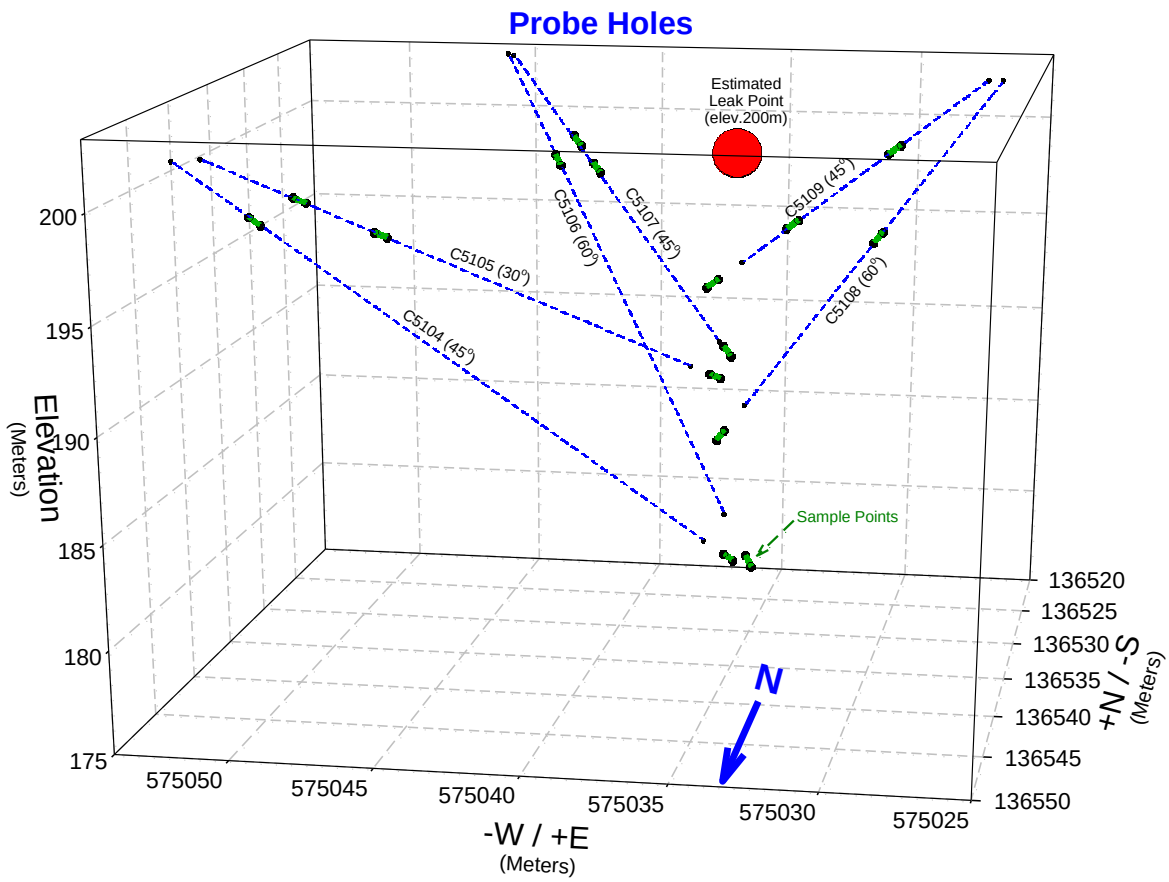

Source: RPP-34643, *Small Diameter Geophysical Logging at the 241-C-152 Diversion Box*.

The geochemistry for the push samples, including slant and vertical pushes, were presented in PNNL-15617. Most appropriate for a comparison with electrical resistivity surveying is the electrical conductivity of the porewater, presented in Tables 4.2 and 4.17 of that report (*ibid.*). A summary of those data, presented graphically, can be seen in Figure 2-8. In general, the data show very low conductivity values, less than 10 mS/cm. For a comparison the BC Cribs and Trenches Site extracted samples with conductivity values in excess of 180 mS/cm.

Figure 2-8. Porewater EC for push samples around UPR-82.

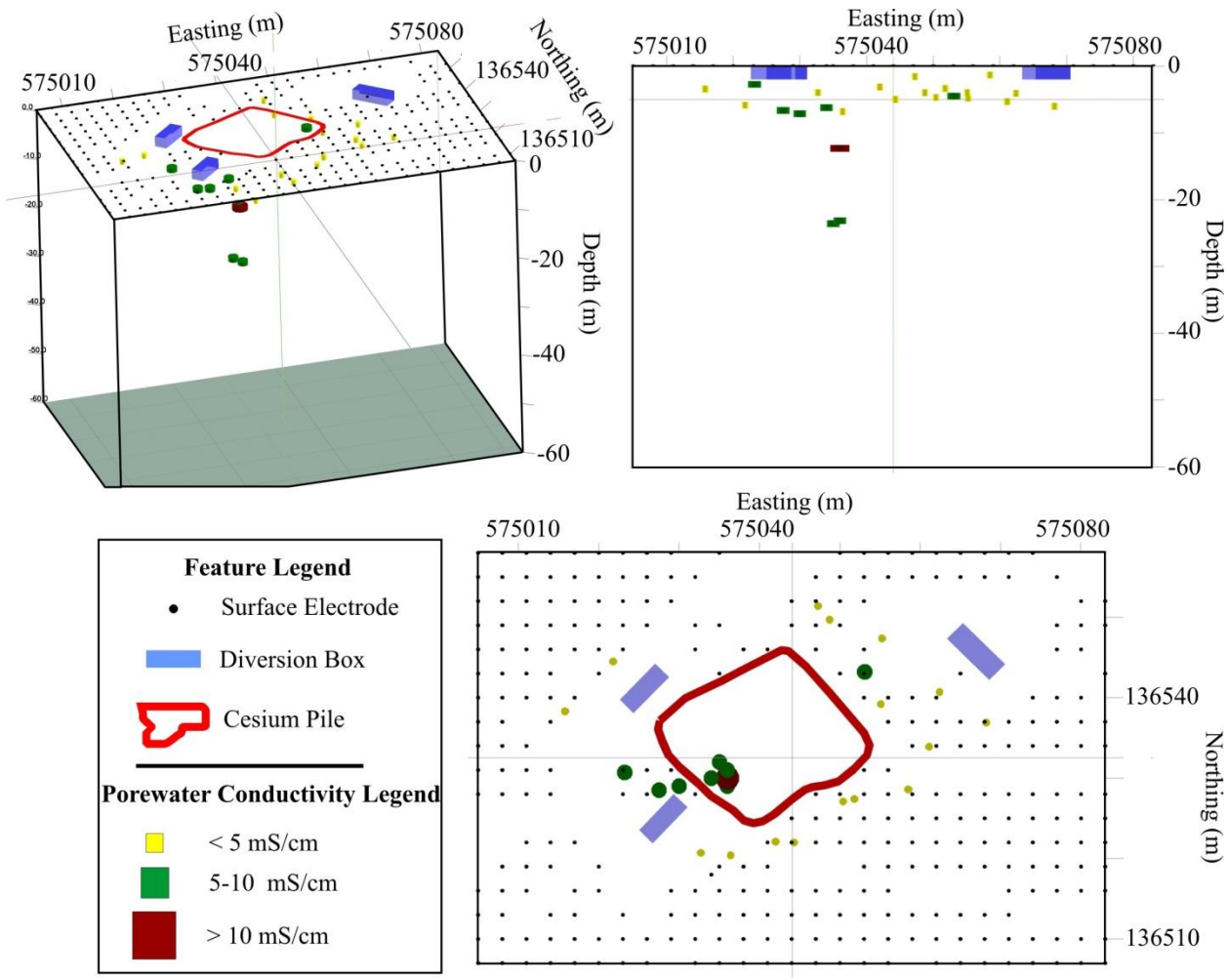

A summary of the conductivity data from PNNL-15617 is presented below:

The second parameter that was assessed to estimate the lateral extent of the leaked plume was the dilution-corrected, water-extraction EC. UPR-200-E-82 is estimated to have contained 1,170 kg sodium, 818 kg nitrate, and 698 kg nitrite (Wood et al. 2003). However, the pore-water-corrected EC data for all of the vertical push samples were dilute and variable, with a range of 1.03 to 6.71 mS/cm. The average pore-water-corrected EC for all 45 vertical push samples analyzed as part of this study was 2.87 mS/cm, which was significantly lower than the average calculated pore-water EC (9.08 mS/cm) in samples from the uncontaminated borehole emplaced north of WMA C (299-E27-22) as part of the C4297 characterization effort, although the sediment samples collected from the 299-E27-22 borehole contained elevated nitrate and were not truly indicative of uncontaminated conditions. Therefore, samples from a study completed near WMA A-AX were used for comparison purposes instead. Two uncontaminated boreholes, emplaced during the construction of groundwater monitoring wells at WMA A-AX, C4665, and C4257, contained average pore-water-corrected conductivities of 1.86 and 2.53 mS/cm, respectively. Based on this, it appears that either 1) there was not a significant lateral spread of

the saline component (i.e., sodium and nitrate) in the C-152 pipeline leak waste plume, or 2) that sufficient hydrologic recharge has occurred to dilute and drive the bulk of the saline components deeper into the vadose zone.

The pore-water-corrected EC data for the slant push samples ranged from dilute (1.22 mS/cm in probe hole C5109) to mildly saline (12.7 mS/cm in probe hole C5105). There was a correlation between elevated pH and EC; the two probe holes containing samples with elevated soil pH (C5105 and C5107) also contained the samples with the highest dilution-corrected pore-water EC. As mentioned in Section 3.1, multiple sample strings (up to 3) were collected from each slant push hole. It is interesting to note that elevated EC was not observed in any of the samples collected within 20 ft of the ground surface. Given that the UPR at this location resulted in the ponding of waste at the ground surface, coupled with the fact that most of the shallow slant push vadose zone samples were collected at or near the edge of the gunite cap, indicates that there was a large vertical transport component for the saline waste components. The elevated pore-water-corrected EC observed in the deepest slant push samples emplaced at this site confirms that dissolved salts (or the saline component of the tank waste stream) have migrated to at least 80 ft bgs.

3.0 DATA ACQUISITION AND PROCESSING METHODOLOGY

Data acquisition for a 3D electrical resistivity survey at the UPR-82 within the C tank farm began on January 21, 2011 and was completed on February 3, 2011. A supplemental 2-dimensional (2D) survey was acquired between April 14, 2011 and April 16, 2011. The geophysical survey acquired electrical resistivity data on a combination of surface electrodes and electrodes buried at variable depths beneath the surface (i.e., depth electrodes). The 3D methodology is in contrast to previous SGE surveys, where data acquisition was relegated to sets of parallel and orthogonal 2D profiles collected along individual lines, which when grouped together produce a pseudo-3D image. A 3D survey is superior to a 2D survey because considerably more data are collected to define the true 3D distribution of electrical properties of the subsurface. However, 3D surveys typically take longer to acquire and require more electrical resistivity equipment.

Data acquisition activities, together with the basis and selection of data acquisition equipment, and data processing steps are described in the following sections.

3.1 SURVEY DESIGN

The resistivity survey was conducted in two phases: Phases A and B. Phase A involved a true 3D data acquisition strategy over a smaller area. Phase B consisted of acquisition of longer 2D profiles centered on the site to gain a better understanding of the conditions near the groundwater.

In Phase A, 3D electrical resistivity data were acquired on 303 surface electrodes, distributed across a site 78 meters by 51 meters. Electrodes were spaced nominally every 3 meters in the east-west and north-south directions. Some positions within this grid were skipped based on proximity to near-surface infrastructure or surface obstructions. Additionally, five boreholes with nested depth electrodes labeled C-7940, C-7941, C-7942, C-7943 and C-5107 were placed opportunistically within the survey area in locations devoid of surface infrastructure. The depth electrode at C-5107 has been used previously in a C tank farm electrical resistivity survey in 2006; this electrode is unique in that it was installed directly beneath the area of surface contamination by drilling at a 45 degree angle from a surface location adjacent to the UPR-82 site. The footprint of the depth electrodes did not necessarily align to the surface electrode grid. Table 3-1 displays the locations and depths associated with each depth electrode.

Phase B data acquisition consisted of three 2D electrical resistivity profiles ranging between 372 meters and 417 meters in length. Each line was centered on the UPR-82 cesium pile with the intent to provide additional information at depth to supplement the 3D coverage.

Figures 3-1 and 3-2 detail the electrode layout for the Phase A and Phase B surveys.

Figure 3-1. Electrode Layout and the Local Distribution of Infrastructure for the UPR-82 3D Survey Area.

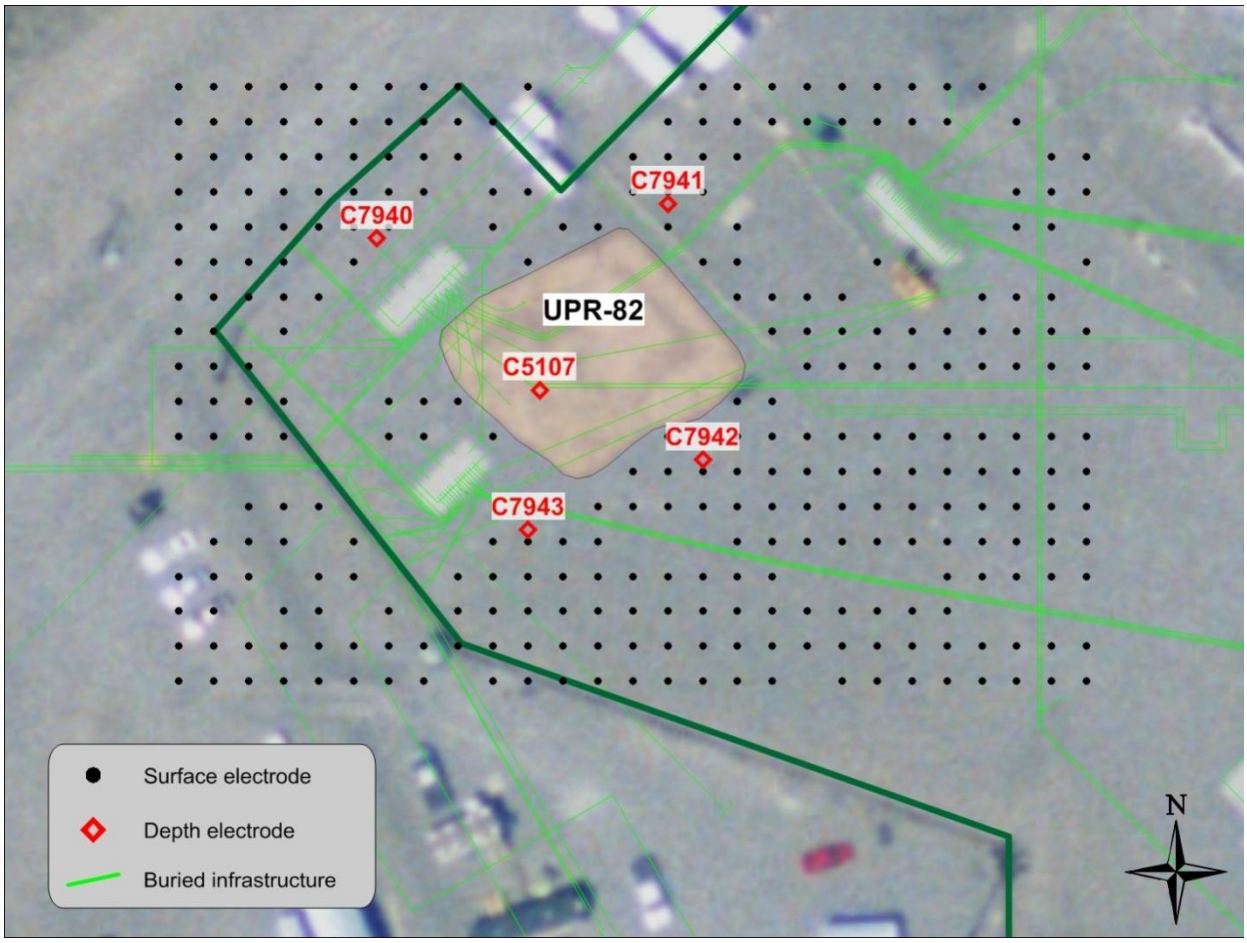

Table 3-1. Depth Electrode Locations. (2 sheets)

Probe Hole #	Electrode #	Northing (m)	Easting (m)	Electrode Depth (m)	Electrode Depth (ft)
C7940	C7940-16	136545.1	575022.1	4.88	16
—	C7940-36	—	—	10.97	36
—	C7940-56	—	—	17.07	56
—	C7940-76	—	—	23.16	76
—	C7940-96	—	—	29.26	96
—	C7940-116	—	—	35.36	116
—	C7940-136	—	—	41.45	136
—	C7940-156	—	—	47.55	156

Table 3-1. Depth Electrode Locations. (2 sheets)

Probe Hole #	Electrode #	Northing (m)	Easting (m)	Electrode Depth (m)	Electrode Depth (ft)
—	C7940-176.5	—	—	53.80	176.5
C7941	C7941-14	136548.2	575046.5	4.27	14
—	C7941-34	—	—	10.36	34
—	C7941-54	—	—	16.46	54
—	C7941-74	—	—	22.56	74
—	C7941-94	—	—	28.65	94
—	C7941-114	—	—	34.75	114
—	C7941-134	—	—	40.84	134
—	C7941-154	—	—	46.94	154
—	C7941-173	—	—	52.73	173
C7942	C7942-16	136526.1	575049.6	4.88	16
—	C7942-36	—	—	10.97	36
—	C7942-56	—	—	17.07	56
—	C7942-76	—	—	23.16	76
—	C7942-96	—	—	29.26	96
—	C7942-116	—	—	35.36	116
—	C7942-136	—	—	41.45	136
—	C7942-156	—	—	47.55	156
—	C7942-176.5	—	—	53.80	176.5
C7943	C7943-16	136520.1	575034.5	4.88	16
—	C7943-36	—	—	10.97	36
—	C7943-56	—	—	17.07	56
—	C7943-76	—	—	23.16	76
—	C7943-96	—	—	29.26	96
—	C7943-116	—	—	35.36	116
—	C7943-135	—	—	41.15	135
C5107	C5107	136532	575036	12	39

Figure 3-2. Electrode Layout for the UPR-82 2D Survey Area.

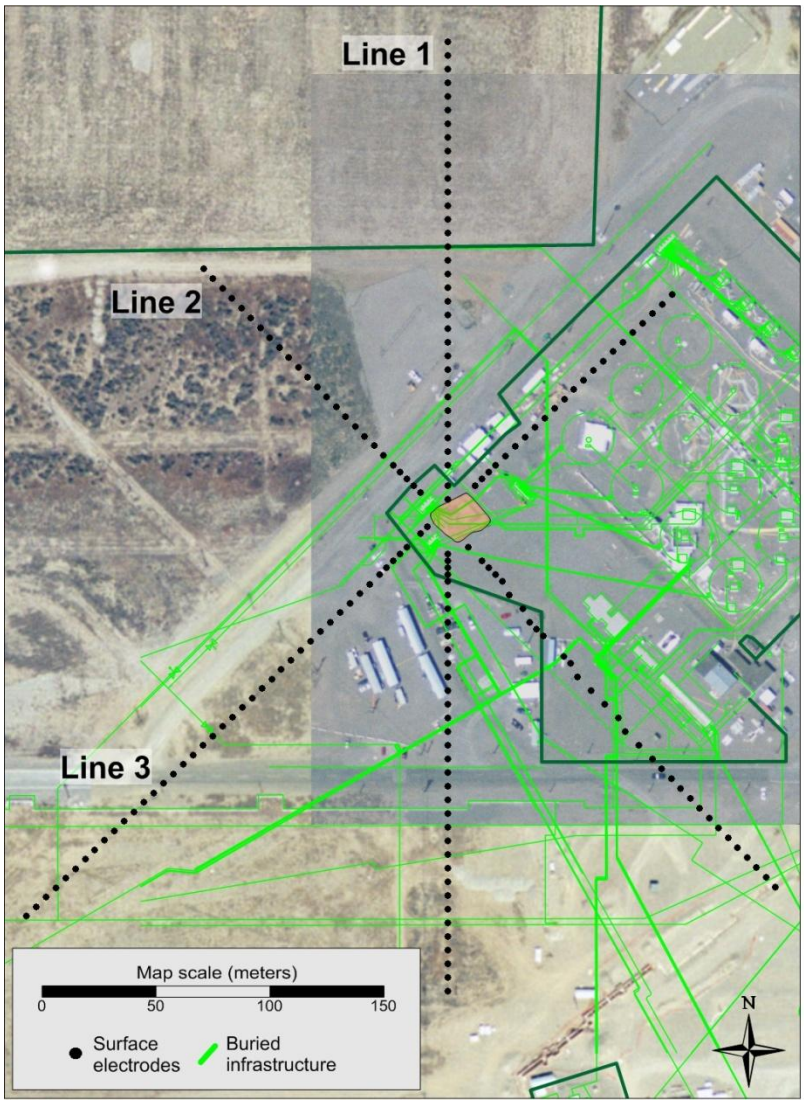

3.2 EQUIPMENT

3.2.1 Electrode and Cable Layout

The first stage of the project was to assemble all available infrastructure maps for the UPR-82 area. The maps containing infrastructure locations, including subsurface pipes/structures and surface structures, were digitized and combined with the preliminary electrode locations. Electrode locations were then modified/omitted to avoid being directly over infrastructure where possible. Electrode placement was limited by maintaining a uniform 3 meter grid layout to support data processing software. The final electrode layout was then uploaded into a Leica®

® Leica is a registered trademark of Leica Technology.

1200 Global Positioning System (GPS), which was used to mark locations on the ground surface. The Leica system has sub-centimeter accuracy, assuring the survey geometry will remain intact.

The electrodes are connected to the electrical resistivity acquisition meter by way of multi-core cables and multiplexors. For the UPR-82 project, a total of four cables were deployed, with each cable allowing up to 84 electrodes to be connected. The cables were arranged in a serpentine pattern, with jumpers connecting the stainless steel probe (electrode) to the multi-core cable. Figure 3-3 shows the cable and electrode layout used for Phase I of this project.

A combination of switch boxes (multiplexors manufactured by AGI) acted as junction boxes to connect the electrical resistivity meter to the multi-core cables. The multiplexors provided capability for addressing 392 electrodes, of which 303 were used for surface electrodes, and 35 for depth electrodes; the remaining nodes were not used for this survey. A separate patch panel was used to connect the depth electrodes to the multiplexors.

Figure 3-3. Resistivity Cable and Surface Electrode Layout.

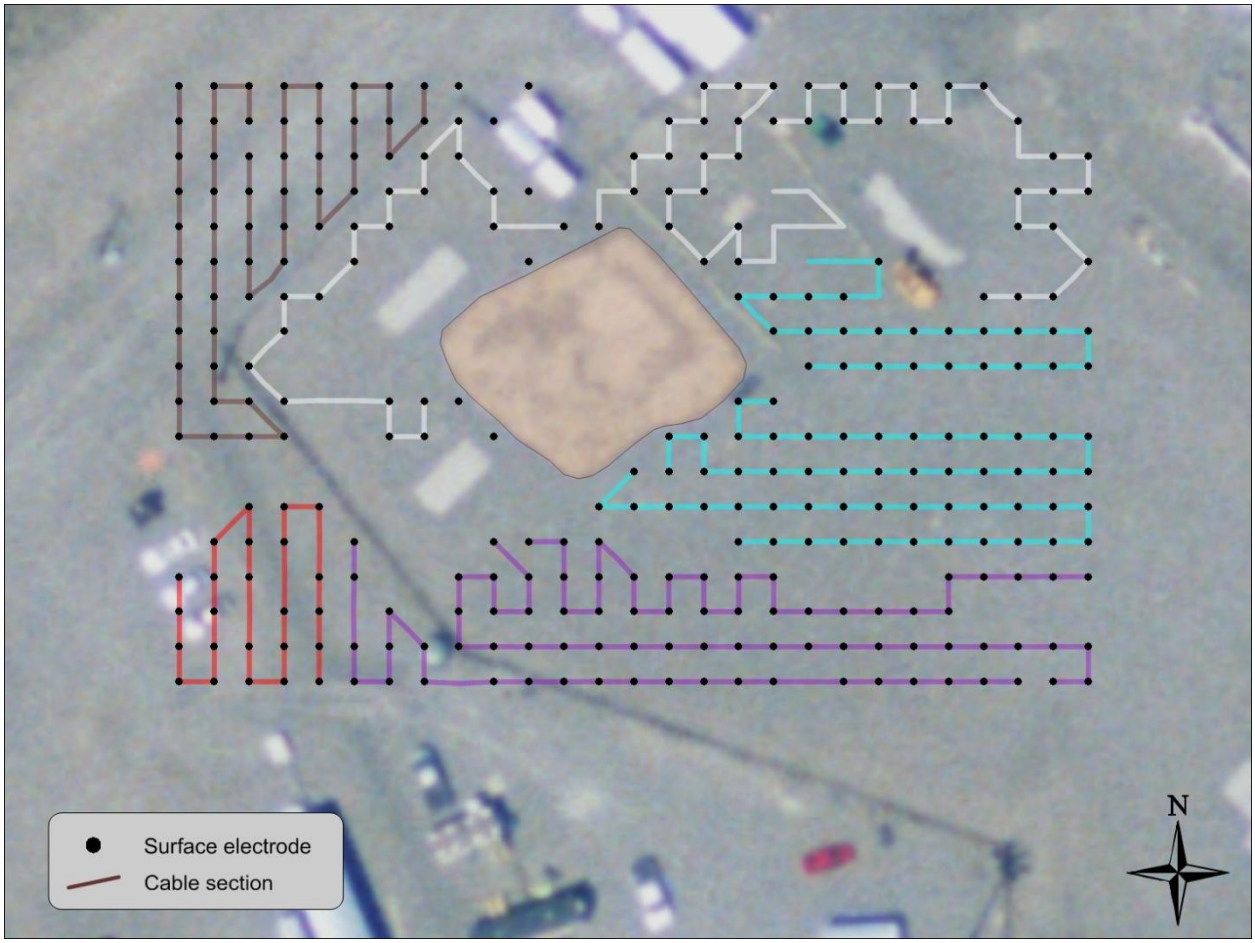

3.2.2 Resistivity Meter

A (SuperSting R8®) electrical resistivity meter, manufactured by AGI, was used for data acquisition. The meter is capable of full 8-channel acquisition, whereby eight simultaneous measurements of voltage can be made during electrical current transmission. The R8 meter has been used for many SGE projects and has proven itself to be reliable for long-term, continuous acquisition campaigns.

Intensive quality assurance was completed before and after the survey to ensure the equipment was functioning appropriately and the data quality was acceptable. Calibration requirements for the hardware used to collect the geophysical data are described in CEES-0360, *Surface Geophysical Exploration System Design Description*. As an example, the manufacturer (AGI) of the Superstong R8 instrument recommends a yearly calibration of internal calibration resistors. The calibration is performed at the manufacturer's facility and a certificate of calibration is provided. A copy of the calibration documentation, serial numbers, and expiration dates are maintained in the project files.

Daily inspection of the receiver calibration was also performed onsite using the manufacturer-supplied calibration resistor test box. The supplied test box is connected to the SuperSting R8 before commencing the daily survey. A specific calibration test firmware is provided within the SuperSting R8 and provides the operator with a pass/fail indication for each of the eight receiver channels. If any of the channels fail, a recalibration or repair is required.

3.3 ACQUISITION METHODOLOGY

The electrical resistivity acquisition used a pole-pole array, where one electrode from each of the transmitting and receiving electrode pairs were placed effectively at infinity. Practically, these poles are placed anywhere from 2 to 5 times the maximum distance between electrodes in the layouts discussed previously, away from the site in opposite directions. Figure 3-4 shows the locations of the remotes used in the 2011 UPR-82 survey, which was different than those used for the UPR-81 and UPR-86 surveys in 2008 and 2010, respectively. For UPR-82, it was necessary to place the remote electrodes further away because the survey area was larger due to the inclusion of the long 2D resistivity profiles.

Phase I 3D data acquisition was initialized on January 21, 2011, and completed February 3, 2011. Data were acquired approximately 18 hours a day to minimize impacts to tank farm operations. Additionally, continuous data acquisition was used to minimize the influence of changing soil moisture conditions over longer periods of time. Personnel were maintained onsite at all times during acquisition to monitor data collection and to keep the cable area clear of vehicles and equipment that could damage cables and impact data quality.

Both forward and reverse data sets were collected during data acquisition in order to increase the confidence of the resistivity survey and evaluate data quality. Forward and reverse measurements are acquired by switching the transmitting and receiving electrodes to produce a reciprocal dataset. The two sets of data ensured that each electrode acted as both transmitter and receiver; both are needed for quality control. The concept of reciprocity in electrical resistivity measurements implies that a homogeneous earth should allow for consistent measurements in

® SuperSting R8 is a registered trademark of Advanced Geosciences, Inc.

both forward and reverse measurement conditions. Thus, by varying selected reciprocal percent difference thresholds, the ratio between data quality and quantity can be assessed. For this survey effort, data measurements with a relative percent difference greater than 5 percent were considered unacceptable and removed from the dataset before numerical inverse modeling.

Phase II 2D data collection was completed between April 14, 2011 and April 16, 2011. Each of the linear profiles required approximately two to three hours of acquisition time, depending on the line length. Additionally, repeat and reciprocal (forward and reverse) data sets were again collected for quality assurance purposes. As during the 3D collection, the survey area was restricted and continuously monitored to protect the equipment and preserve data quality.

Figure 3-4. Remote Locations.

3.4 DATA PROCESSING

3.4.1 3D Data Reduction

All raw data collected at the site were compiled into a relational database. Raw data included both electrical resistivity data and GPS positional data to geo-reference the electrical resistivity data. A set of queries was designed to segregate reciprocal pair data points and assign each data point distinguishing characteristics not retained in the raw sting file. This information included electrode type and a sequential electrode number (as designated in the survey design). Additional data fields were added for the calculated distance between electrodes and percent error between reciprocal data. The data were then exported from the database for graphical filtering and plotting in a spreadsheet.

Four important diagnostic data parameters from the raw data include voltage/current (V/I; resistance) ratio, repeat error, reciprocal error, and electrical current output. The repeat

error is a calculated percent error between cycled/repeated measurements. A plot of these data can provide information with regards to the statistical variation of the data population.

The process of data editing identifies and eliminates data points, but no data modification (rounding, averaging, smoothing, or splining) is permitted. The rationale is to seek out and remove spurious points that do not conform to the data population, or points that violate potential theory. The first step in this editing process was to remove data outside of the statistical population – negative V/I, noise, high instrument error, low current, low voltage, etc. Figure 3-5 shows the 3D survey raw data distribution for the forward and reverse measurements, while Figure 3-6 shows the same datasets after filtering. The next step in data reduction was to apply a data quality filter based on reciprocity. All data with a reciprocal percent difference greater than 5 percent was removed.

Figure 3-5. 3D - Forward and Reverse Data Sets (Raw Data).

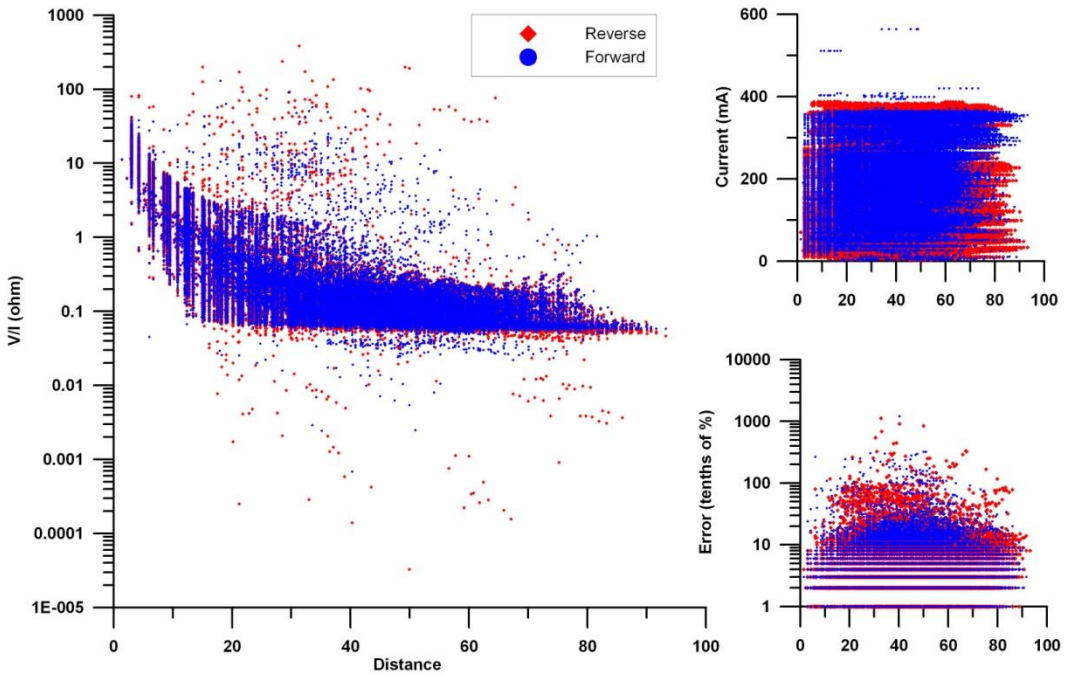

Raw data distribution for (1) V/I (left), (2) Error, and (3) Current (lower right).
All are plotted against the distance between transmitting/receiving electrode pairs.

Figure 3-6. 3D - Forward and Reverse Data Sets after Data Editing.

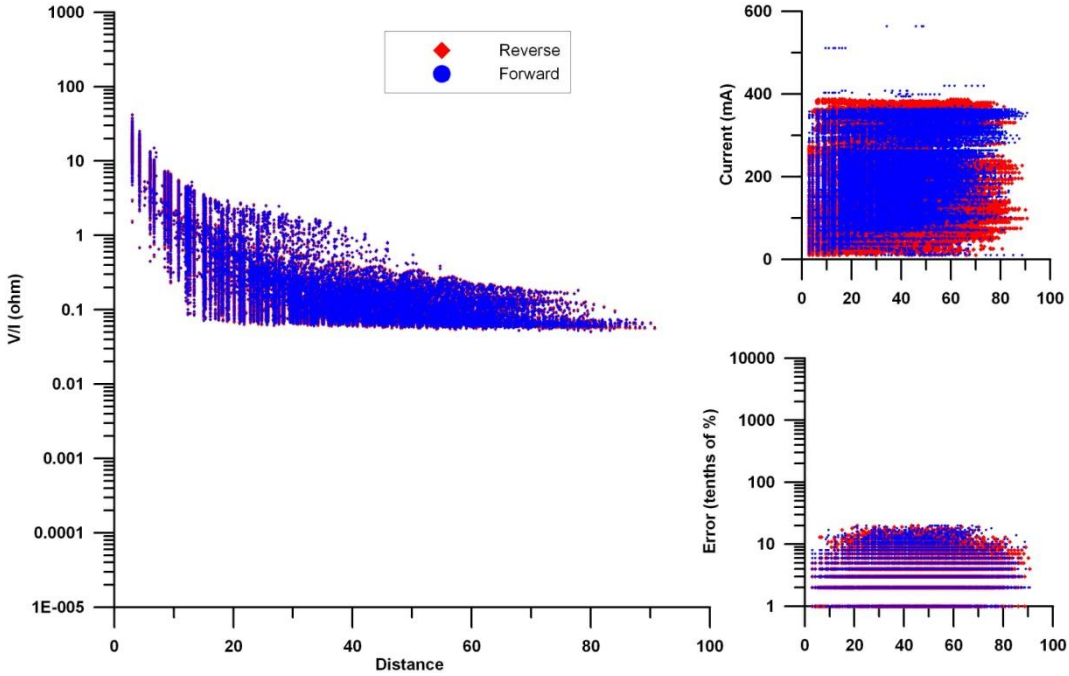

Data distribution after Editing for (1) V/I (left), (2) Error, and (3) Current (lower right).
All are plotted against the distance between transmitting/receiving electrode pairs.

Table 3-2 displays the percentages of data removed or retained during steps of the editing process for the 3D data set.

Table 3-2. 3D - Number of Data Points Retained During Data Editing Steps.

	Forward	Reverse	Sum	Percent of Total
Total Raw	65,330	57,637	122,967	100
Total Combined Reciprocal	57,849*	57,849*	115,698	94.1
Total Edited (<5% Reciprocal Error)	39,860	39,860	79,720	64.8

*NOTE: Some data points were re-collected in the forward and/or reverse data sets resulting in multiple reciprocal data pairs for the same electrode combination.

3.4.2 Depth Electrode Performance

Given the low density of depth electrodes at a given site, where typically 4 to 24 electrodes are placed below ground surface (compared to hundreds of electrodes on the surface), it is important to have maximum performance from all depth electrodes. The current UPR-82 project is an exception, where a total of 35 depth electrodes were installed and used for acquisition. Table 3-3 lists the construction and completion details for the depth electrodes.

Table 3-3. Construction Details for UPR-82 Depth Electrodes.

Electrode Name	***C5107***	***C7940***	***C7941***	***C7942***	***C7943***
Construction Type	Single-probe	Multi-Probe, WRPS	Multi-Probe, WRPS	Multi-Probe, WRPS	Multi-Probe, WRPS
Date of Construction	4/06	10/10	10/10	10/10	10/10
Depth of Probes (ft)	39	16, 36, 56, 76, 96, 116, 136, 156, 176.5	14, 34, 54, 74, 94, 114, 134, 154, 173	16, 36, 56, 76, 96, 116, 136, 156, 176.5	16, 36, 56, 76, 96, 116, 135
Construction Details	Slant-hole installation. Single stainless steel rod electrode, 2 ft long, 0.5 inch diameter. 16 gauge wire connection to the surface.	Stainless steel braids encircling the main cable and exposed at selected depths along the electrode string. An old WRPS rod electrode was used at the bottom of the string.	Stainless steel braids encircling the main cable and exposed at selected depths along the electrode string. An old WRPS rod electrode was used at the bottom of the string.	Stainless steel braids encircling the main cable and exposed at selected depths along the electrode string. An old WRPS rod electrode was used at the bottom of the string.	Stainless steel braids encircling the main cable and exposed at selected depths along the electrode string. An old WRPS rod electrode was used at the bottom of the string.
Fill Material	Unknown, but likely silica sand and saline water surround probe, bentonite fill. Similar to other electrodes of the time.	Sand (20-40) and diatomite surround moisture probe, water added through tremie. Fill of bentonite, sand and diatomaceous earth.	Sand (20-40) and diatomite surround moisture probe, water added through tremie. Fill of bentonite, sand and diatomaceous earth.	Sand (20-40) and diatomite surround moisture probe, water added through tremie. Fill of bentonite, sand and diatomaceous earth.	Sand (20-40) and diatomite surround moisture probe, water added through tremie. Fill of bentonite, sand and diatomaceous earth.

The performance from the different types of electrodes can be explored through output current, repeat error, reciprocal error, and the percentage of voltage data that are negative. Table 3-4 lists the summary statistics from each of these electrodes. Using a cut-off value of 240 milliamp (mA) for average transmitting current, the majority of the depth electrodes are usable. In addition, the average repeat errors are quite low indicating consistent measurements. The average reciprocal error appears to be a better discriminator for bad electrodes. A couple of electrodes in the C7943 have an excessive amount of recorded negative values.

Table 3-4. Depth Electrode Statistics for UPR-82.

Electrode Name	Location	Probe Depths (ft)	Moisture Content (vf%)	Average Transmitting Current (mA)	Average Repeat Error (as Rx) (%)	Percentage of Negative V/I Values	Average Reciprocal Error (% difference)	Percentage of Data Below 5% Error Cut-off
C5107	UPR-82	41	3	172	0.1	3	0.4	100
C7940	UPR-82	16	3	342	0.2	0	0.8	97
		36	2	342	0.1	0	0.6	100
		56	3	301	0.1	3	0.5	100
		76	3	334	0.1	0	0.2	100
		96	3	332	0.1	0	0.2	100
		116	2	343	0.1	6	0.1	100
		136	4	332	0.1	6	0.2	100
		156	3	329	0.1	6	0.2	100
		176	2	183	0.1	6	0.2	100
C7941	UPR-82	14	14	346	0.3	6	0.3	100
		34	3	237	0.1	6	0.2	100
		54	4	331	0.1	3	0.2	100
		74	4	333	0.1	3	0.2	97
		94	4	337	0.1	6	0.1	100
		114	5	347	0.1	5	0.2	100
		134	4	347	0.1	5	0.1	100
		154	4	348	0.1	8	0.2	100
		173	3	348	0.1	5	0.2	100
C7942	UPR-82	16	5	339	0.2	6	0.8	97
		36	3	274	0.2	6	0.9	97
		56	5	344	0.1	6	0.3	100
		76	3	340	0.1	6	0.3	100
		96	4	356	0.1	6	0.7	94
		116	5	352	0.1	6	1.1	97
		136	4	351	0.1	6	0.2	100
		156	6	343	0.1	6	0.3	100
		176	5	352	0.1	6	0.2	100
C7943	UPR-82	16	4	334	0.3	0	3.0	80
		36	4	30	0.1	82	42.4	50
		56	4	248	0.1	76	71.9	0
		76	5	345	0.1	0	0.3	100
		96	4	342	0.1	0	0.4	100
		116	9	355	0.1	0	0.4	100

A performance measure can be computed for each individual depth electrode by summing the number of times each electrode passes the cut-off measure for the four statistics highlighted above. Figure 3-7 shows the performance measure for all of the electrodes, which can take on values of {0, 1, 2, 3, 4}. It would be reasonable to assess good performance with a 3 or 4,

marginal performance with a 2, and poor performance with a 0 or 1. In most cases the electrodes perform well with values of 3 and 4.

Figure 3-7. Performance Measure for Each of the Depth Electrodes.

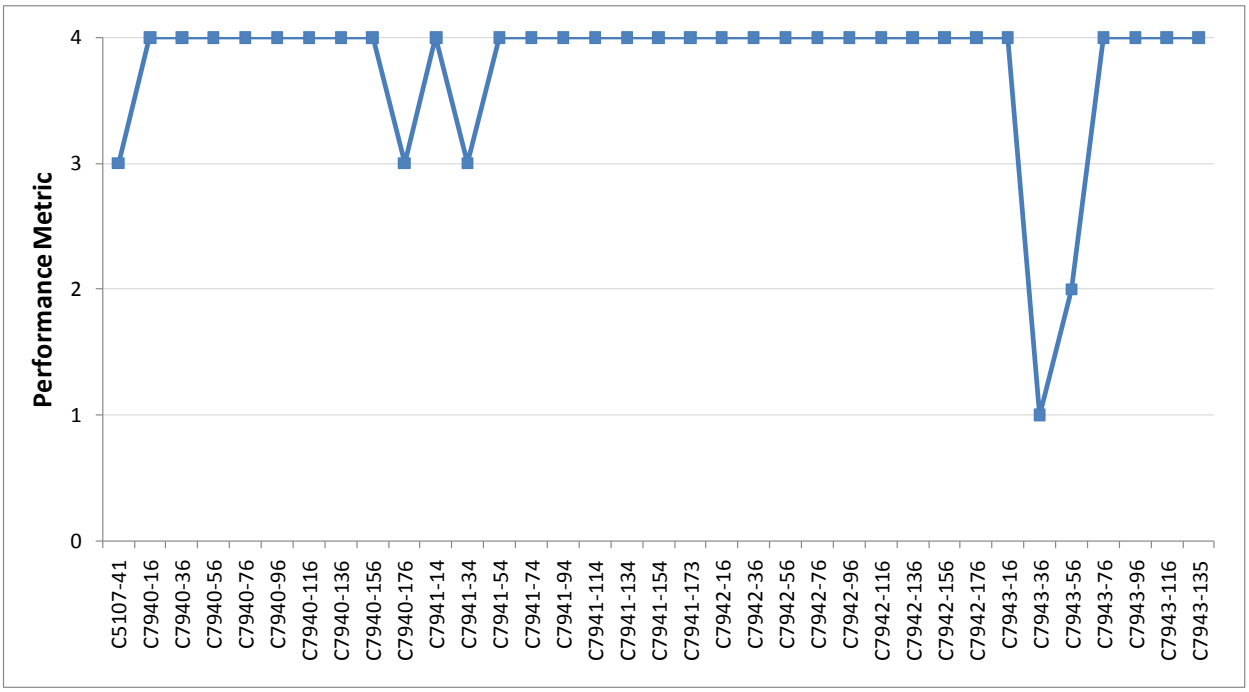

NOTE: Performance of 0 or 1= Poor. Performance of 2 = Marginal. Performance of 3 or 4 = Good.

3.4.3 Depth Electrode Data

A comparison of transfer resistance data collected on the depth electrodes from multiple projects, including BY West, BY East, and the SX tank farms, is presented in Figure 3-8. The data are plotted as a function of distance between transmitter electrode and receiver electrode. Interestingly, the data from UPR-82 appears to have a higher transfer resistance data than the other projects. High transfer resistance translates to higher electrical resistivity. The high electrical resistivity is likely due to the absence of a significant amount of ionic constituents or moisture in the subsurface. The analytical geochemistry results presented in Section 2.0 showed that the highest electrical conductivity porewater is approximately 12 mS/cm, low compared to other tank farms

Figure 3-8. Transfer resistance (V/I) from depth electrodes for multiple projects.

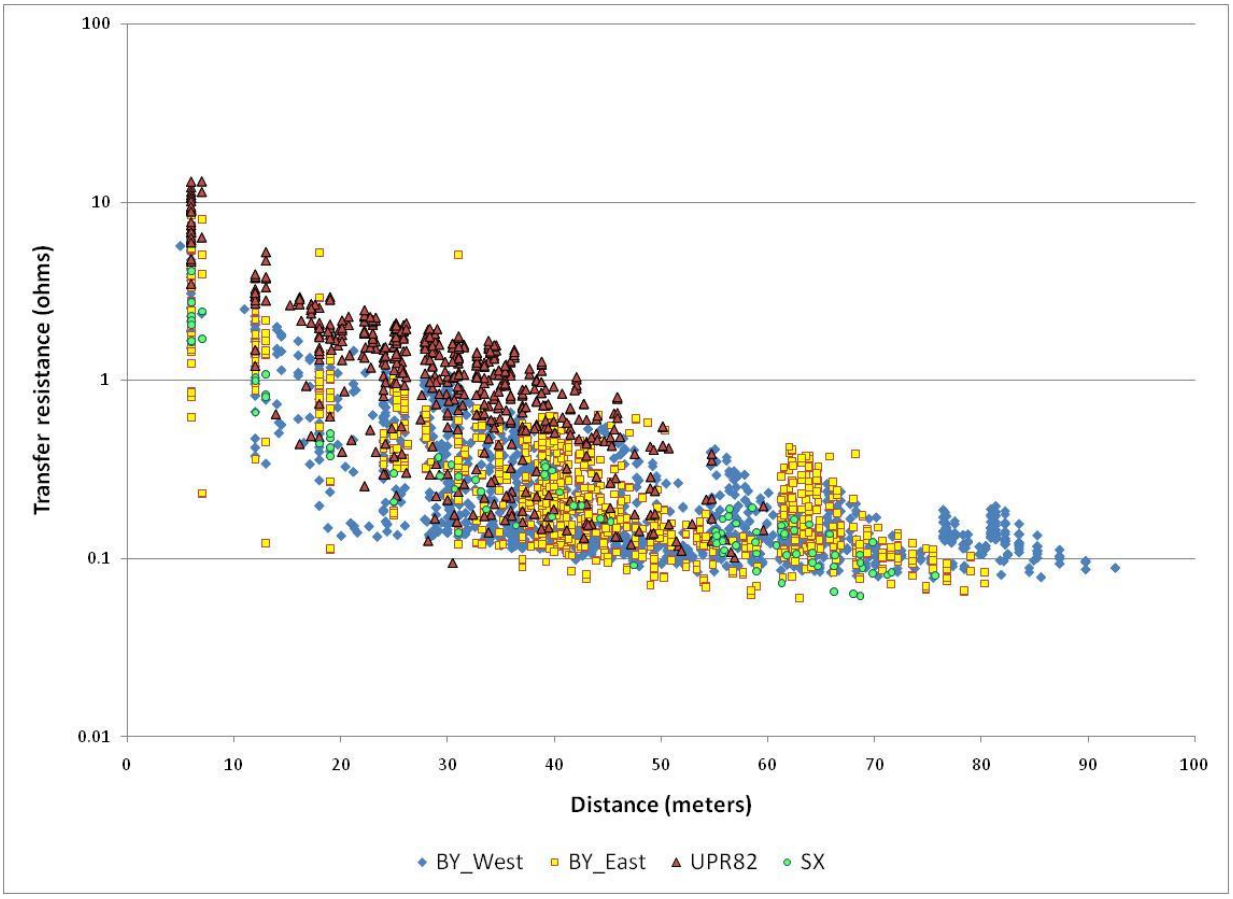

3.4.4 2D Data Reduction

The 2D data acquired at UPR-82 were placed into spreadsheets and, as with the 3D data, evaluated in order to seek out and remove spurious data points. Data parameters assessed include apparent resistivity, normalized potential (V/I), repeat error, and electrical current. In general, criteria for data removal are data points which do not conform to the surrounding data population, or data points that conflict with potential theory. Figure 3-9 shows examples of the types of data that would be targeted for removal in the data filtering process. Table 3-5 highlights the actual filtering statistics for the UPR-82 2D lines. Line 2 appears to have a significantly lower quality data set, with over 31% of the data removed. This may be due to a higher presence of interference from subsurface infrastructure in the tank farm.

Figure 3-9. 2D Data Filtering Example.

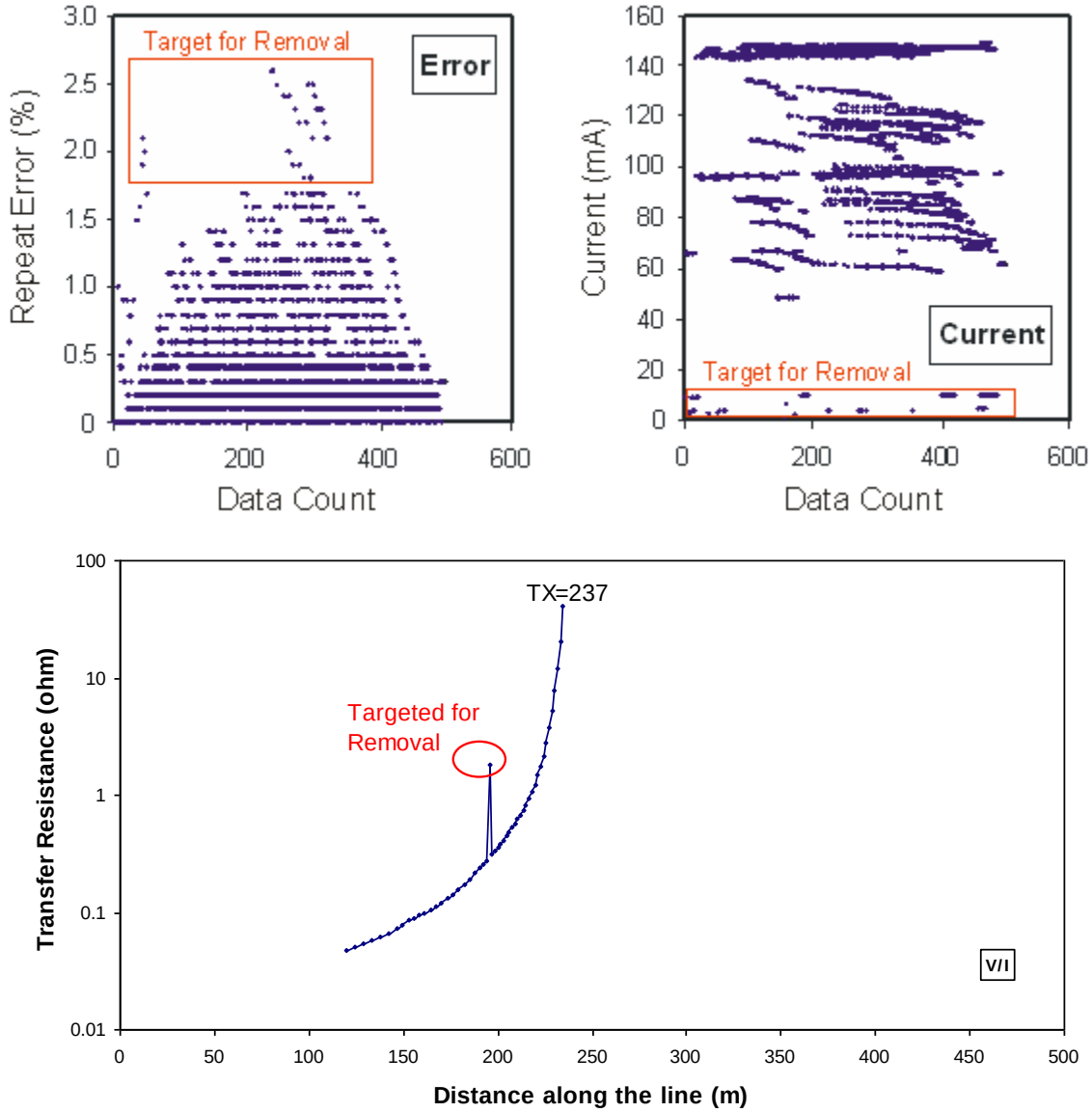

Table 3-5. Data Reduction Statistics for the UPR-82 2D Resistivity Lines.

Line	No. Data Points (Raw)	No. Data Points (Filtered)	No. Data Points Removed	% Data Removed
Line 1-Forward	2,346	2,324	22	0.94
Line 1-Reverse	2,344	2,306	38	1.62
Line 2	1,387	952	435	31.36
Line 3	1,793	1,691	102	5.69

A comparison of the forward and reverse data sets for Line 1 was used as a secondary basis for evaluating data quality by evaluating the error between reciprocal data pairs. When data with a reciprocal percent difference greater than 5 percent are removed, 1,981 of the original 2,344 reciprocal pairs remain (84.5% retention). Figure 3-10 shows a plot of the normalized potential values for the forward and reverse data sets acquired along Line 1.

Figure 3-10. Line 1 Normalized Potential (V/I).

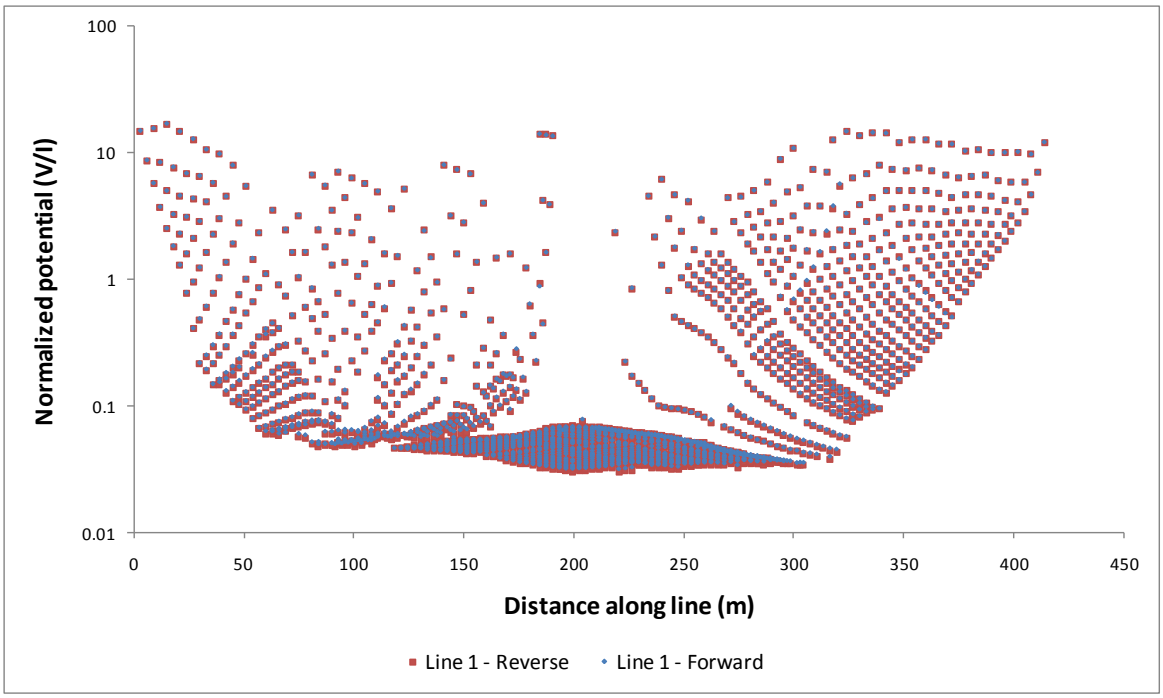

3.4.5 Inverse Modeling

Popular use of the RES2D and RES3D series of resistivity inversion codes has led both professional and academic users to regard these codes as industry standard software. The UPR-82 modeling effort used RES2DINV and RES3DINVx64, a 64-bit multi-threaded version developed specifically for a large number of electrodes.

In general, inverse modeling can be summarized in the following five steps:

1. The study site's voltage data has been measured and is discretized into grid nodes using a finite difference or finite element mesh. The meshing parameters used in either case, to design the computational grids, are dependent on electrode spacing used in site-specific data acquisition.

2. The inversion will set out to estimate the true resistivity at every grid node. An initial estimate of the subsurface properties is made based on the literal translation of the pseudo-section to a true resistivity, a constant value, or some other distribution from *a-priori* information. A forward model run with these initial estimates is made to obtain the distribution of voltages in the subsurface. The root-mean-square (RMS) error is calculated between the measured voltage and the calculated voltage resulting from the forward run.

3. Based on the degree of model fit to field measurements, the initial estimate of resistivity is changed to improve the overall model fit and the forward model with the updated estimates is rerun. The iterative method linearizes a highly nonlinear problem using Newton's method. Using this method, the inverse modeling code essentially solves the linearized problem to obtain the change in modeled resistivity (Δm) for the next iteration.

4. The resistivity model is updated using the general formula $m_{i+1} = m_i + \Delta m$, where $_{mi+1}$ is the resistivity in a model cell at the next iteration, and m_i is the current value.

Steps 3 and 4 are repeated until the RMS error change between successive iterations reaches an acceptable level

4.0 MODELING RESULTS

Upon completion of data filtering, measured apparent resistivity data from the UPR-82 site were inverse modeled using the RES3DINVx64 software package for the 3D data, and the RES2DINV software package for the 2D data. For specific details of the SGE resistivity method and theoretical basis applied to inverse modeling, the reader is referred to discussions provided in RPP-34690, *Surface Geophysical Exploration of the B, BX, and BY Tank Farms at the Hanford Site*.

To accomplish the 2D and 3D inversions, every surface and depth electrode were geo-referenced (using the Washington State Plane – Meters coordinate system) to allow absolute placement of an electrode within the inversion algorithm. The model was then run with a set of input parameters that have been demonstrated to work well in tank farm environments.
After inversion, the final results from the inversion models were interpolated to a regular grid and visualized using the Rock Works™ visualization software package and Surfer® surface contouring package. The visualization allows discrimination of low resistivity targets that could be associated with increased moisture, increased ionic strength of the pore water, infrastructure, or a combination of these items. It is anticipated that mineralogy and porosity would have minimal effects on the resistivity outcome.

4.1 3D POINT ELECTRODE MODELING

The point electrode data modeling initially included measurements from 303 surface electrodes and 35 depth electrodes. Not all of the data was of acceptable quality, and some data or measurements associated with particular electrodes were removed from the model data set to reduce errors. To create the final datasets for inversion, two types of data reduction occurred between the data acquisition and final plotting phases. First, data quality was inspected to eliminate unacceptable data that may have resulted from instrumentation error, electrical interference, or high data misfit with respect to neighboring points. The process of removing spurious data points is referred to as editing and is performed prior to the first inversion run. Second, data were filtered after each inverse model was completed to remove data points that contributed to a high model RMS error. This process is referred to as a filter run, and the objective of a filter run was to reduce the final RMS to an acceptable level. Each model was assigned a model number which designated a specific data set or set of modeling parameters and each filter run was assigned a successive random number. An example label for a model with a filter run is “Model_001i.”

The 3D model focused on the highest quality measured resistivity data by removing those data with repeat errors greater than 2 percent and reciprocal errors greater than 5 percent. After noisy data removal, 39,860 data values remained for inclusion in the model. After completing two filtering runs to remove additional spurious data, 35,560 data remained. Table 3-2 lists the

™ Rock Works is a trademark of Rockware, Inc
® Surfer is a registered trademark of Golden Software, Inc.

statistics for the modeling and Figure 3-6 shows how the data are distributed in a transfer resistance vs. distance plot.

As with any numerical model, a mesh was created whereby the subsurface was discretized into blocks and nodes. The equations that describe the potential field during electrical current transmission are then solved at every node with the appropriate boundary conditions. RES3DINVx64 automatically generates the mesh for these forward model calculations by placing four grid lines between each electrode for a finely discretized mesh. Additional requirements of the numerical model include explicitly assigning every block an initial resistivity value and every node a current source (if any).

For the inverse modeling, where the resistivity values are changed in the model domain to match measured and modeled voltages as closely as possible, a separate mesh was created that did not perfectly replicate the forward model mesh. The arbitrary gridding for the inverse model prevented very small cells from being created due to the positions of the borehole electrodes not being aligned to the surface electrode grid. We chose a square 3 m grid cell for the inverse model, which created 28 cells in the x-direction and 19 cells in the y-direction. The model extended to a depth of 72m below ground surface. Figure 4-1 shows the 3 m grid used for modeling UPR-82.

Figure 4-1. Inverse model grid used for modeling the UPR-82 site.

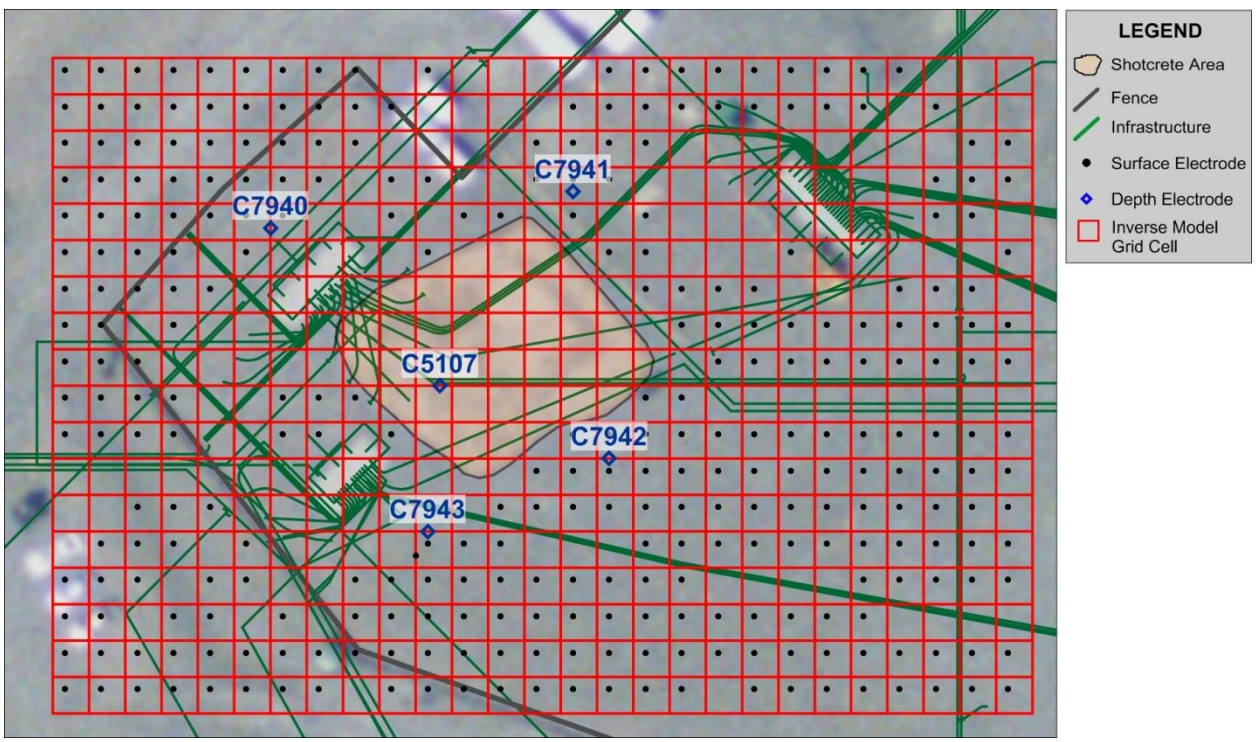

The final pieces of information entered into the inverse model input file were subsurface layers representing the infrastructure in the top two meters and a resistive earth for the remaining 70 meters of the model. These data were entered as *a priori* information due to initial testing of the model, and it was found that a value of 20 ohm-m for the top two meters and a value of 1,000

ohm-m for the bottom resistive layer were best. The RES3DINVx64 code also permits the user to assign a confidence rating to the data using integers from 1 to 10. One is the lowest confidence rating and simply suggests to the model that this is a place to start for finding the best resistivity solution, while 10 is used to hold data values as absolute in the modeling routine. For the UPR 82 modeling we provided a value of 1 for the confidence rating.

The results of the inverse modeling are shown in Figure 4-2. The figure was constructed from the output file for the fifth iteration of the second filtered model run and shows slices at select depths within the model domain. The depths are indicated in the upper left corner of each plot within the mosaic. Furthermore, pipelines are traced in green to show their effects on the final resistivity distribution and the shotcrete boundary placed over the cesium pile is shown for reference.

Figure 4-2. Plan View Depth Slices of Calculated Resistivity for Filtered Dataset.

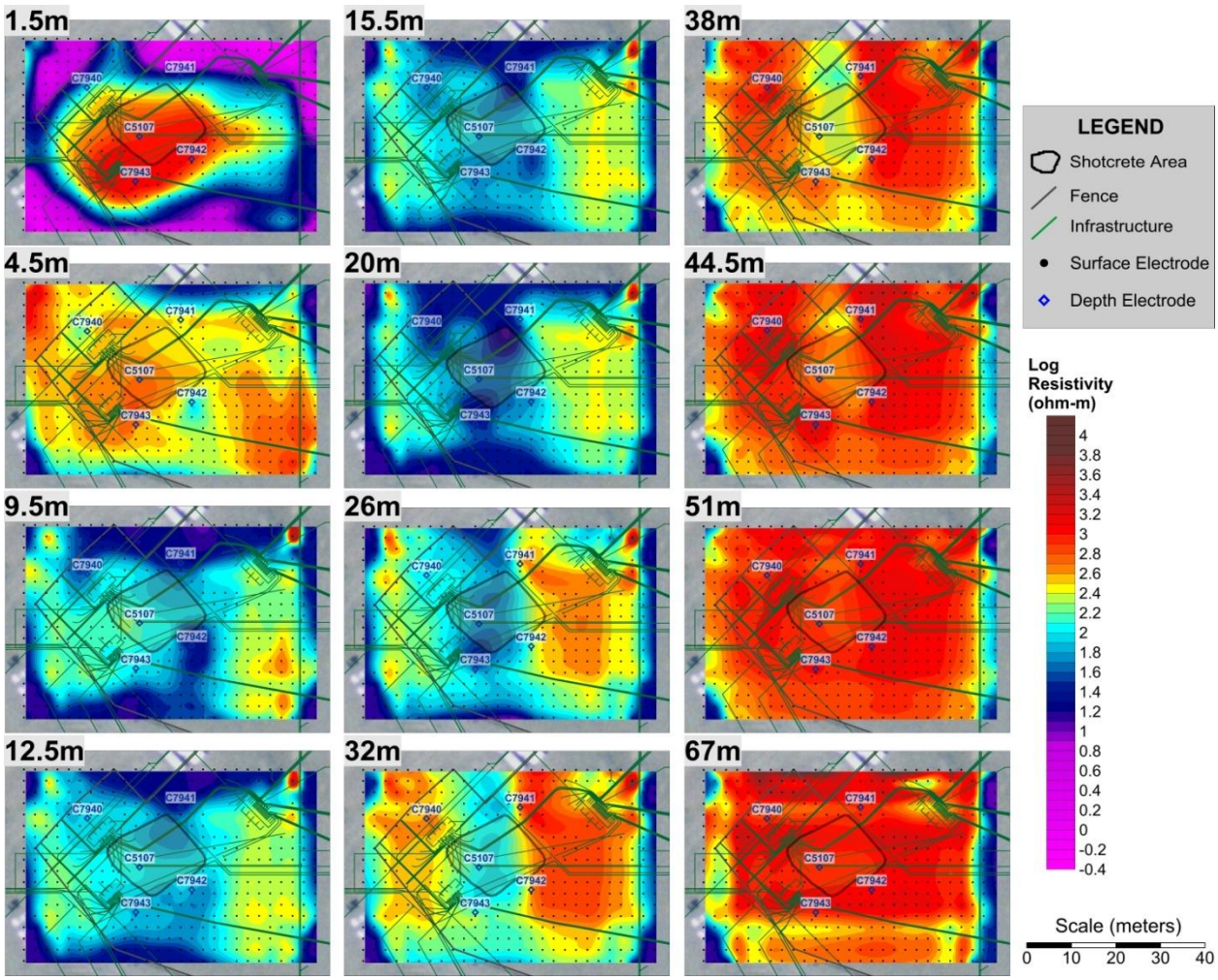

The top model layer and the side boundaries of the majority of the model layers display the most conductive features, with values less than 10 ohm-m around the periphery. In contrast, the

internal regions of the top model layer display significantly higher resistivity values. By 4.5 m depth, the resistivity increases slightly towards the boundaries, with values between 100 and 1,000 ohm-m. The four layers between depths of 9.5 and 20 m display generally lower values of resistivity; the variability in the upper portion of the model may be caused by variability in soil moisture. The lower portion of the model, below 20 m, displays an increase in resistivity as the vadose zone becomes drier as indicated in PNNL-15617.

In general, there does not appear to be a specific low resistivity signature associated with the UPR-82. The sampled porewater data from the various direct pushes indicates low electrical conductivity, which may be too low in this instance to image with electrical resistivity. Similar results were observed to the south for the UPR-86 site, where the resistivity method found no discernable targets that could be associated with a release. In Figure 4-1 there are some seemingly low resistivity features below the cesium pile. The values, are roughly 100 ohm-m which is significantly higher than other resistivity targets associated with past releases. Lastly, the raw resistance data from the depth electrodes were significantly higher than other similar projects where significant depth electrode data existed. The higher depth electrode resistance values suggest that overall the subsurface is electrically resistive. A lack of ionic porewater, such as nitrate, sulfate, or chloride, combined with a generally dry soil would produce a resistive ground.

Figure 4-3 displays a three-dimensional rendering of the resistivity material beneath the shot-create covered cesium pile. This is represented as an isometric view of the region, as viewed from the southwest (towards the north east). Two levels of resistivity values are presented, with the small opaque resistivity body in green (resistivity value of 225 ohm-m) and the larger transparent resistivity body in blue (resistivity value of 175 ohm-m). To place these isopleths in context to other recent work, the rendered bodies for the resistivity features in BY west, that were associated with past releases, were 0.5 and 1.0 ohm-m. Figure 4-2 suggests no discernable resistivity feature exists associated with the release at UPR-82.

Figure 4-3. 3D rendered resistivity values at UPR 82 (view from southwest).

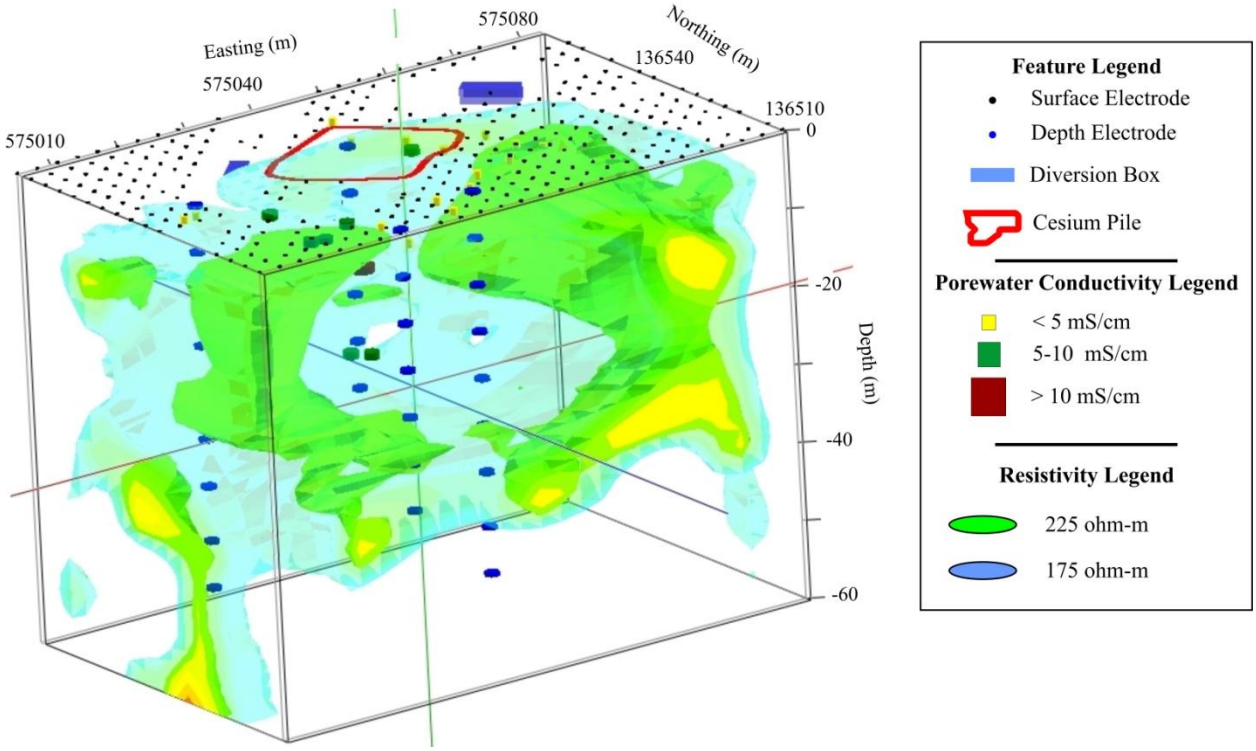

4.2 2D RESISTIVITY MODELING

The 2D data modeling was completed using measurements acquired from surface electrodes along the three linear profiles of Line 1, Line 2, and Line 3. The survey lines were designed to be centered over the UPR-82 target, with Line 1 oriented in the north-south direction and Lines 2 and 3 rotated to headings of approximately 45 and 315 degrees, respectively. Additionally, to ensure consistency and quality control during the field data acquisition, the lines were designed to use the same equipment set – five cable sections of 28 electrode takeouts giving a maximum capacity of 140 electrodes at 3 meter spacing and line length of 417 meters. A nominal electrode spacing of 6 meters was used due to the considerable length of the survey lines, and existing electrodes from the UPR-81, UPR-82, and UPR-86 3D survey grids were used wherever possible.

The 2D modeling process followed a similar procedure to the 3D modeling. A data reduction routine first eliminated poor performing electrodes and data that were deemed unacceptable, which may have resulted from instrumentation error, electrical interference, or high data misfit with respect to neighboring points. In addition, data were filtered after each inverse model was completed to remove data points that contributed to a high model RMS error. This process is referred to as a filter run, and the objective of a filter run was to reduce the final RMS to an acceptable level. However, this error based filtering did not always improve the model; the RMS error remained relatively high in Lines 2 and 3. Modeling statistics are presented below in Table 4-1.

Table 4-1. 2D Inverse Model Statistics.

Line	Number of Electrodes	Length (m)	Array Type	Number of Inversion Filter Runs	Number of Iterations	Final Model RMS Error (%)
Line 1	69	417	Forward + Reverse	1	7	4.95
Line 2	51	371	Reverse	1	5	16.21
Line 3	64	394	Reverse	0	6	12.18

Final results for the 2D inverse modeling are presented in Figures 4-4 through 4-6. In an effort to display the features of this data relative to the observed surface infrastructure in an aerial photo, the profiles have been rotated out of the vertical plane that they represent and into the horizontal plane of the aerial photo. The photo of the survey area shows the electrode locations as well as pipelines and other tank farm infrastructure. Resistivity values are presented in a logarithmic scale, with lower values shown as cool hues (pink, blue) and higher values in warm hues (red, brown).

In general, higher resistivities are noted in the background material outside the tank farm area (at the beginning and end of each line) and low resistivities are observed around the target area (near the center of each line). However, the low resistivity responses seen in all of the profiles are indicative of a significant amount of interference from metallic infrastructure. The method of presentation highlights this extremely well. A low resistivity feature emanates from the surface at nearly every instance of infrastructure, particularly near the center of each line where the highest concentration of infrastructure is found. Interference from individual pipelines tends to be additive due to their close proximity to one another. Consequently the interference overwhelms the model, making the data virtually impossible to decipher in terms of the impact of the past release at UPR-82.

Figure 4-4. Line 1 2D Inverse Model.

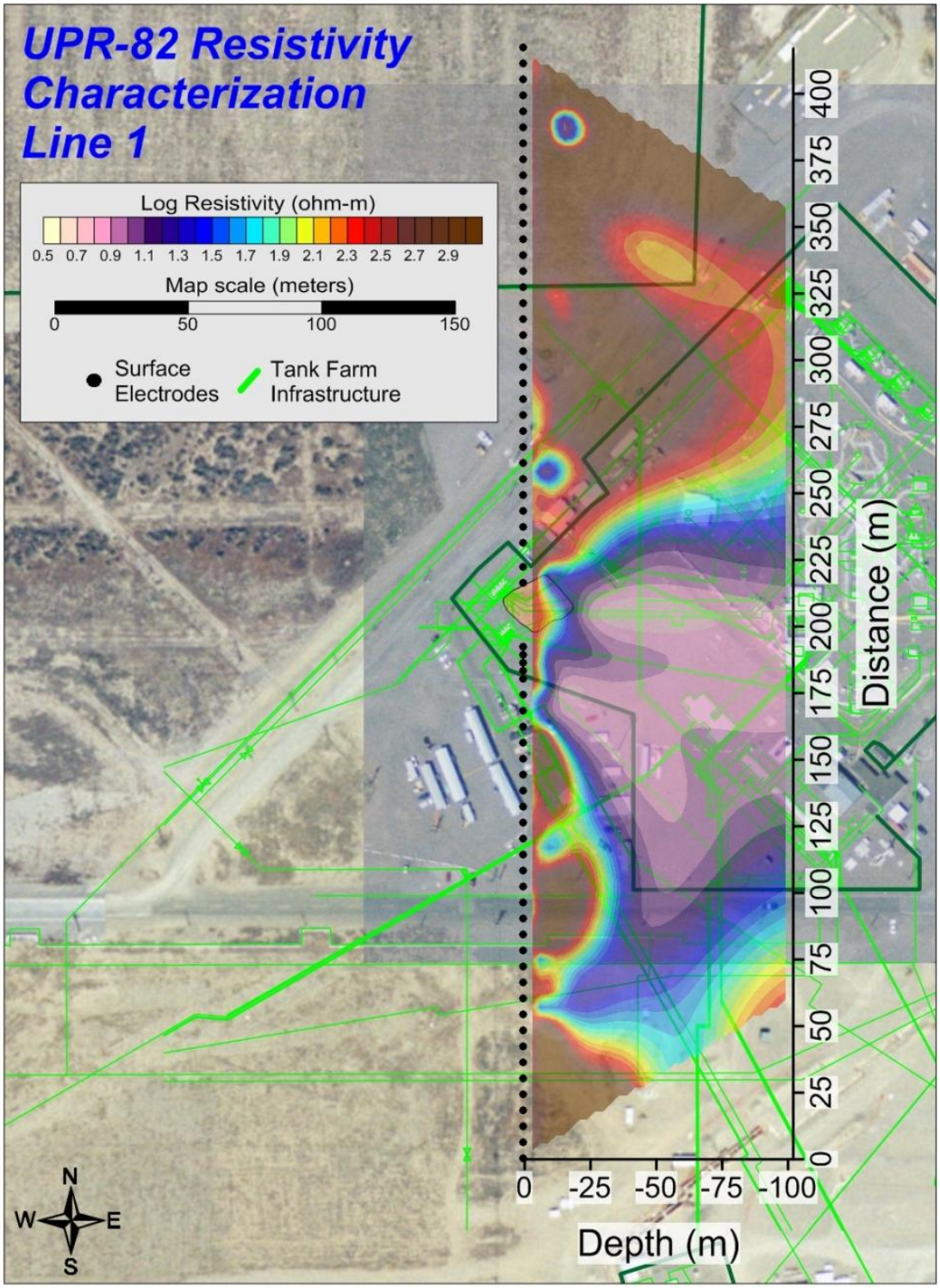

Figure 4-5. Line 2 2D Inverse Model.

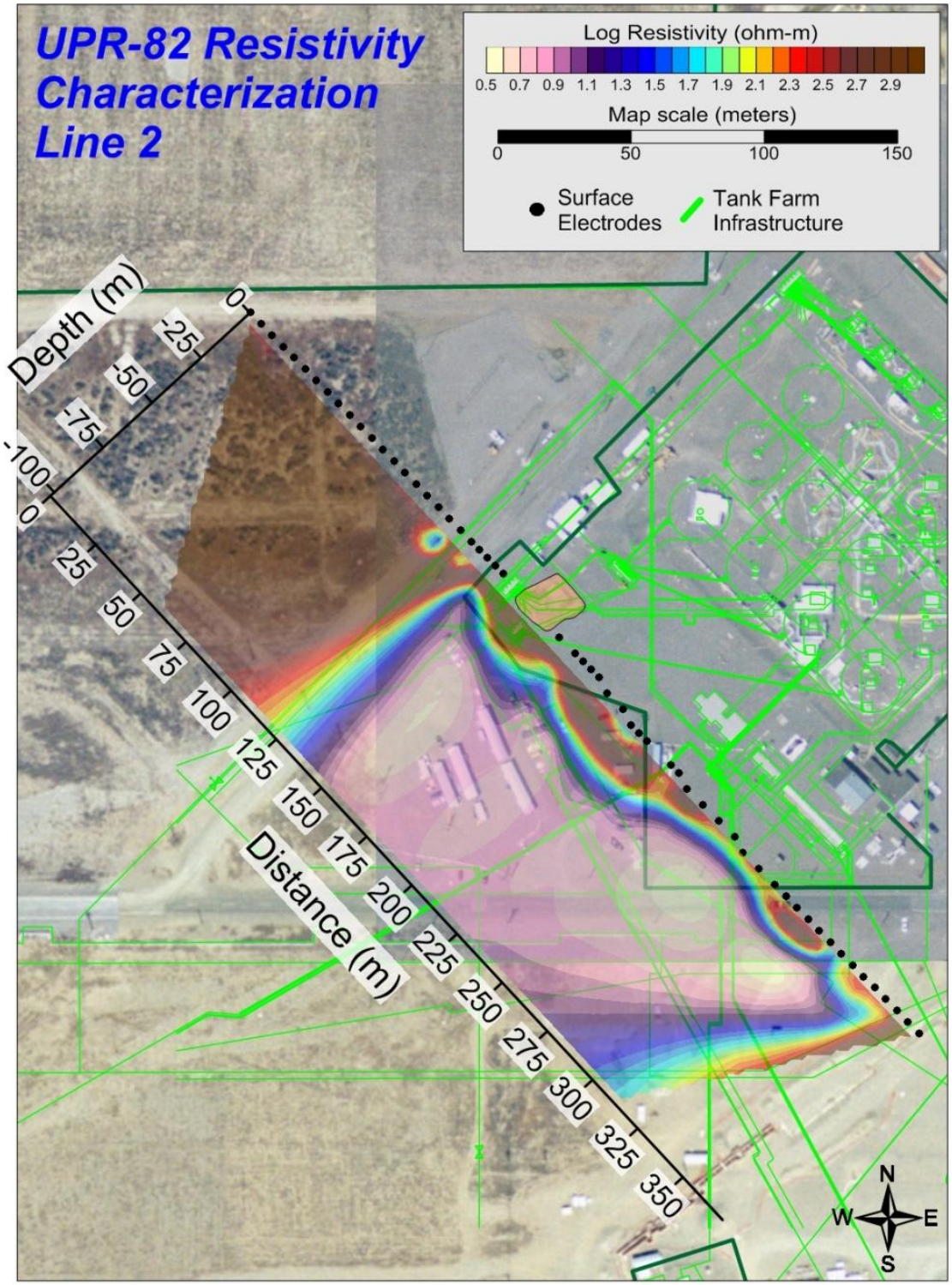

Figure 4-6. Line 3 2D Inverse Model.

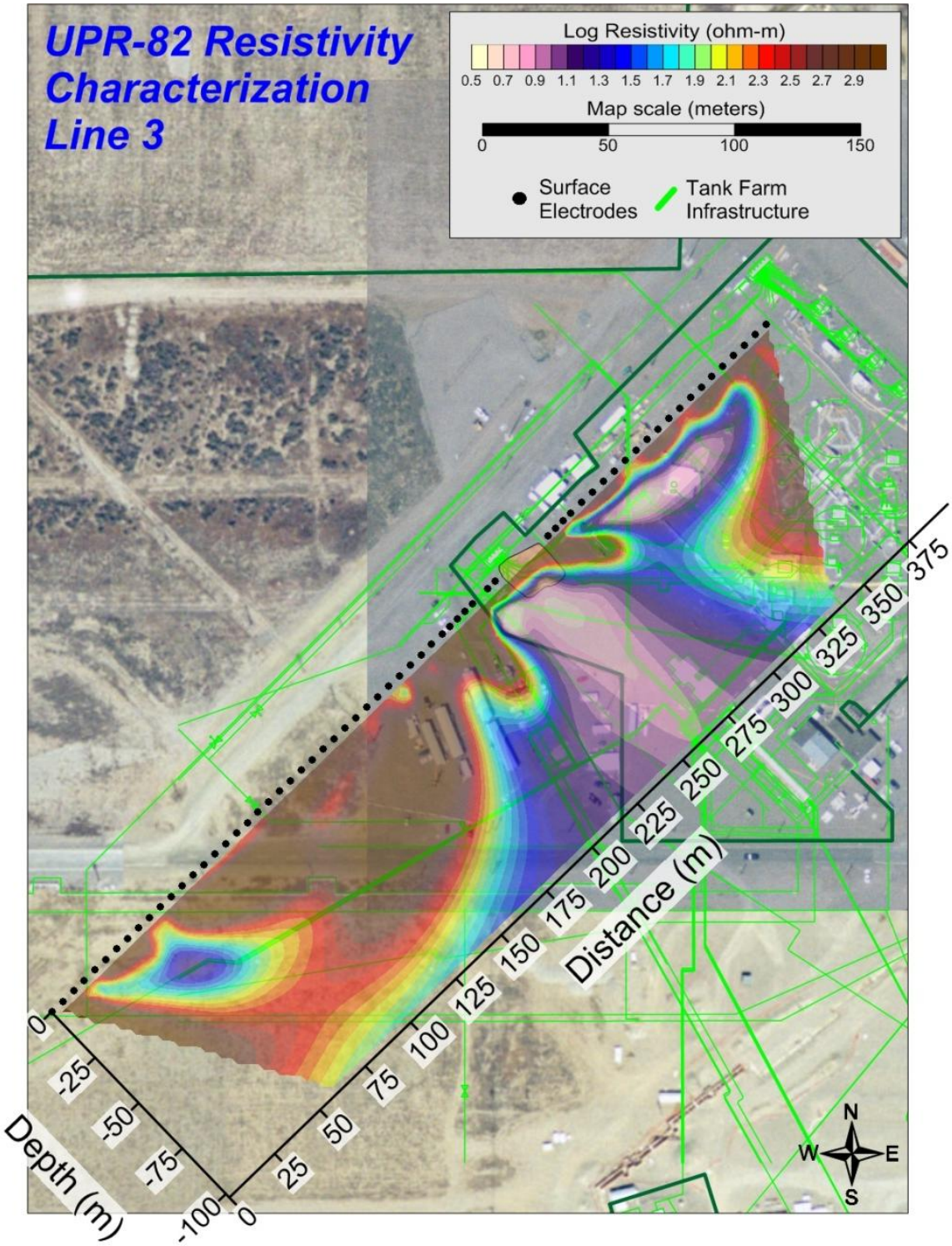

5.0 CONCLUSIONS

A SGE survey was conducted over the UPR-82 release within the C tank farm on the Hanford Site. The survey focused on imaging the extents of the past release directly beneath the cesium pile. The survey included a concentrated 3D analysis, with measurements on 303 surface electrodes placed within a grid and 35 depth electrodes in five boreholes, and a 2D survey with three profile lines extending outside of the UPR-82 and C tank farm.

The inverse models were conducted with a concentrated 3D dataset using high quality surface and depth electrode data. The results of the model showed a general distribution of high electrical resistivity values beneath the UPR-82 release, with values approximately two orders of magnitude higher than other sites where a discernable feature was noted in the resistivity data. Two other lines of evidence besides the 3D model suggest that the soil is, in fact, electrically resistive. The first is the raw depth electrode transfer resistance data, which showed generally higher values than other sites, including BY west, BY east, and SX tank farm. The other is the sampled soil data and analytical results from the direct pushes around the region. Although a maximum porewater electrical conductivity value of 12 mS/cm was observed beneath the UPR-82 site, this target was too small and of too low intensity to be imaged by the resistivity method, even with the high contrast between expected target values and background values. Other sites, where resistivity has been extremely successful, display much higher porewater EC. The conclusion, is that the spill at UPR-82 was either of low volume and not a source of groundwater contamination for the waste management area, or actions taken to control exposure to the spill have resulted in it being diluted and/or flushed into the underlying groundwater. The size of the UPR-82 release, 2600 gallons, favors the former interpretation. There is no evidence in the resistivity data to indicate that the UPR has been mis-located or that other releases may have taken place.

The second survey included a set of three long profile lines centered over the UPR 82 release to gain an understanding of potential groundwater impacts from the site. Unfortunately, the surface data were significantly impacted by the near surface infrastructure and no meaningful information could be discerned from the model results. For example, the low resistivity features aligned with known infrastructure at the site, which then reduced resolution and masked effects of any other potential targets.

6.0 REFERENCES

ARH-LD-132, *Geology of the 241-C Tank Farm*, Atlantic Richfield Hanford Company, Richland, Washington.

CEES-0360, 2007, *Surface Geophysical Exploration System Design Description*, Revision 0, Columbia Energy and Environmental Services, Inc., Richland, Washington.

DOE/RL-2008-01, 2008, *Hanford Site Groundwater Monitoring for Fiscal Year 2007*, Revision 0, U.S. Department of Energy, Richland, Washington.

HNF-EP-0182, 2009, *Waste Tank Summary Report for Month Ending April 30, 2009*, Washington River Protection Solutions, LLC, Richland, Washington.

HW-61780, *Subsurface Geology of the Hanford Separation Areas*, General Electric, Co Hanford Atomic Products Operation, Richland, Washington.

PNNL-14656, 2004, *Borehole Data Package for Four CY 2003 RCRA Wells 299-E27-4, 299-E27-21, 299-E27-22, and 299-E27-23 at Single-Shell Tank, Waste Management Area C, Hanford Site, Washington*, Pacific Northwest National Laboratory, Richland, Washington.

PNNL-15070, 2005, *Hanford Site Groundwater Monitoring for Fiscal Year* 2004, Pacific Northwest National Laboratory, Richland, Washington.

PNNL-15617, 2008, *Characterization of Vadose Zone Sediments from C Waste Management Area: Investigation of the C-152 Transfer Line Leak*, Revision 1, Pacific Northwest National Laboratory, Richland, Washington.

PNNL-15670, *Hanford Site Groundwater Monitoring for Fiscal Year 2005*, Pacific Northwest National Laboratory, Richland, Washington.

PNNL-15837, *Data Package for Past and Current Groundwater Flow and Contamination Beneath Single-Shell Tank Waste Management Areas*, Pacific Northwest National Laboratory, Richland, Washington.

PNNL-15955, *Geology Data Package for the Single-Shell Tank Waste Management Areas at the Hanford Site*, Pacific Northwest National Laboratory, Richland, Washington.

PNNL-16346, *Hanford Site Groundwater Monitoring for Fiscal Year 2006*, Pacific Northwest National Laboratory, Richland, Washington.

RPP-14430, 2003, *Subsurface Conditions Description of the C and A-AX Waste Management Area*, Revision 0, CH2M HILL Hanford Group, Richland, Washington.

RPP-15317, 2003, *241-C Waste Management Area Inventory Data Package*, Revision 0, CH2M HILL Hanford Group, Richland, Washington.

RPP-16608, 2004, *Site-Specific Single-Shell Tank Phase 1 RCRA Facility Investigation/Corrective Measures Study Work Plan Addendum for Waste Management Areas C, A-X, and U*, Revision 1, CH2M HILL Hanford Group, Inc., Richland, Washington.

RPP-19866, 2004, *Calculation for the Post-Retrieval Waste Volume Determination for Tank 241-C-106*, Revision 1, CH2M HILL Hanford Group, Inc., Richland, Washington.

RPP-23748, 2006, *Geology, Hydrogeology, Geochemistry, and Mineralogy Data Package for the Single-Shell Tank Waste Management Areas at the Hanford Site*, Revision 0, CH2M HILL Hanford Group, Inc., Richland, Washington.

RPP-34643, 2007, *Small Diameter Geophysical Logging at the 241-C-152 Diversion Box*, Revision 0, CH2M HILL Hanford Group, Inc., Richland, Washington

RPP-34690, 2007, *Surface Geohphysical Exploration of the B, BX, and BY Tank Farms at the Hanford Site*, Revision 0, CH2M HILL Hanford Group, Inc., Richland, Washington.

RPP-35484, 2008, *Field Investigation Report for Waste Management Areas C and A-AX*, Revision 1, CH2M HILL Hanford Group, Inc., Richland, Washington.

RPP-PLAN-39114, 2011, *Phase 2 RCRA Facility Investigation/Corrective Measures Study Work Plan for Waste Management Area C*, Revision 1B, Washington River Protection Solutions, LLC, Richland, Washington.

RPP-PLAN-39364, 2010, *Work Plan for Surface Geophysical Exploration of UPRs near the C Tank Farm*, Revision 1, Washington River Protection Solutions, LLC, Richland, Washington.

RPP-RPT-41236, 2009, *Surface Geophysical Exploration of UPR 200-E-81 Near the C Tank Farm*, Revision A, Washington River Protection Solutions, LLC, Richland, Washington.

RPP-RPT-42294, 2010, *Hanford Waste Management Area C Soil Contamination Inventory Estimates*, Revision 1, Washington River Protection Solutions, LLC, Richland, Washington.

RPP-RPT-47486, 2010, *Surface Geophysical Exploration of UPR 200-E-86 Near the C Tank Farm Resource Conservation and Recovery Act of 1976*, Revision 0, Washington River Protection Solutions, LLC, Richland, Washington.